ESDU 86010
Issued October 1986
With Amendments A to E
August 2001

Characteristics of atmospheric turbulence near the ground
Part III: variations in space and time for strong winds (neutral atmosphere)

ESDU DATA ITEMS

Data Items provide validated information in engineering design and analysis for use by, or under the supervision of, professionally qualified engineers. The data are founded on an evaluation of all the relevant information, both published and unpublished, and are invariably supported by original work of ESDU staff engineers or consultants. The whole process is subject to independent review for which crucial support is provided by industrial companies, government research laboratories, universities and others from around the world through the participation of some of their leading experts on ESDU Technical Committees. This process ensures that the results of much valuable work (theoretical, experimental and operational), which may not be widely available or in a readily usable form, can be communicated concisely and accurately to the engineering community.

We are constantly striving to develop new work and review data already issued. Any comments arising out of your use of our data, or any suggestions for new topics or information that might lead to improvements, will help us to provide a better service.

THE PREPARATION OF THIS DATA ITEM

The work on this particular Data Item was monitored and guided by the Wind Engineering Panel. This Panel, which took over the work on wind engineering previously monitored by the Fluid Mechanics Steering Group, first met in 1979 and now has the following membership:

Chairman

Mr T.V. Lawson	—	Bristol University

Members

Mr C.W. Brown	—	Freeman Fox Ltd
Prof. J.E. Cermak*	—	Colorado State University, USA
Dr N.J. Cook	—	Building Research Establishment
Mr D.D. Croft	—	Ove Arup and Partners
Prof. A.G. Davenport*	—	University of Western Ontario, Canada
Dr D.M. Deaves	—	Atkins Research and Development
Dr A.R. Flint	—	Flint and Neill
Prof. D.H. Freeston*	—	Auckland University, New Zealand
Mr R.I. Harris	—	Cranfield Institute of Technology
Prof. K.C. Mehta*	—	Inst. for Disaster Research, Texas Tech. Univ., USA
Mr R.H. Melling	—	Racal Antennas Ltd
Dr W. Moores	—	Meteorological Office
Dr G.A. Mowatt	—	Earl and Wright Ltd
Mr J.R.C. Pedersen	—	Independent
Mr C. Scrutton	—	Independent
Mr R.E. Whitbread	—	British Maritime Technology Ltd
Mr G. Wiskin	—	British Broadcasting Corporation.

* Corresponding Members

The technical work involved in the assessment of the available information and the construction and subsequent development of the Data Item was undertaken by

Mr N. Thompson	—	Group Head, Wind Engineering

The person with overall responsibility for the work in this subject area is Mr N. Thompson, Head of Wind Engineering Group.

CHARACTERISTICS OF ATMOSPHERIC TURBULENCE NEAR THE GROUND PART III: VARIATIONS IN SPACE AND TIME FOR STRONG WINDS (NEUTRAL ATMOSPHERE)

CONTENTS

CHARACTERISTICS OF ATMOSPHERIC TURBULENCE NEAR THE GROUND
Part III: variations in space and time for strong winds (neutral atmosphere)

1. NOTATION* AND UNITS

		SI	*British*
a_{ii}	decay constant in exponent of Equation (7.5) for $\gamma_{ii}(\Delta r)$		
$C_{ii}\{r,r';\tau\}$, $C_{ii}\{\Delta r\}$	cross-covariance function; time averaged value of product $i\{r;\ t\} \cdot i\{r';\ t+\tau\}$	m^2/s^2	ft^2/s^2
f	longitudinal correlation function, see Equation (5.5)		
g	lateral correlation function, see Equation (5.6)		
h	gradient height, *i.e.* height of upper edge of Earth's boundary layer; see Section 3	m	ft
$i\{r;\ t\}, i$ $j\{r;\ t\}, j$	general value of gust component at point r or r' and time t where $i, j = u$, v or w	m/s	ft/s
${}^{r}L_i$	general length scale of i-component of turbulence in direction of r (see Section 6)	m	ft
${}^{x}L_u$, ${}^{y}L_v$, ${}^{z}L_w$	principal longitudinal length scales of turbulence measured along $r = x$, y or z axis respectively (see Section 6)	m	ft
n	frequency	Hz	Hz
$P\{i,j\}$, $p\{i,j\}$	joint-probability and joint-probability density functions respectively (see Section 4)	s^2/m^2	s^2/ft^2
$P_{ii}\{\underline{r},\ \underline{r}';\ n\}$, $P_{ii}\{\Delta r\}$	co-spectral density function, in-phase component of $S_{ii}\{\Delta r\}$	m^2/s	ft^2/s
$Q_{ii}\{r,\ r';\ n\}$, $Q_{ii}\{\Delta r\}$	quad-spectral density function, out-of-phase component of $S_{ii}\{\Delta r\}$	m^2/s	ft^2/s
$r\ ;\ r'$	position vectors denoting points (x, y, z) and (x', y', z') respectively	m	ft
$\tilde{r}_f$	longitudinal non-dimensional separation when Δr is in direction of i-component; $\Delta r / {}^{r}L_i$		

* For notational convenience, the dependency of the various cross-correlation and cross-spectral functions on the relative spatial location of the points $(x, y, z,)$ and (x', y', z') is denoted by Δr; in practice the various functions are also dependent on $z_m = \frac{1}{2}(z + z')$. Also, the functional dependence on τ or n is dropped from the notation used in the main text.

Issued October 1986
Reprinted with Amendments A to E, August 2001 – 32 pages
This page Amendment E

$\tilde{r}_g$	lateral non-dimensional separation when Δr is normal to direction of i-component; $\Delta r/(2^{r}L_i)$		
Δr	distance separating points r and r'; $(\Delta x^2+\Delta y^2+\Delta z^2)^{½}$	m	ft
Δr_e	equivalent separation distance for non-zero time lag; $((\tau V_m+\Delta x)^2+\Delta y^2+\Delta z^2)^{½}$	m	ft
Δs_i	component of Δr_e resolved in direction in which gust component i is acting	m	ft
$S_{ii}\{n\}, S_{ii}$	single point spectral density function	m^2/s	ft^2/s
$S_{ii}\{r, r'; n\}$, $S_{ii}\{\Delta r\}$	cross-spectral density function	m^2/s	ft^2/s
t	time	s	s
u, v, w	fluctuating or gust components of wind speed along x, y and z axes respectively	m/s	ft/s
V_m	average of hourly-mean wind speed at points r and r'; $V_m \approx V_z$ at $z = z_m$	m/s	ft/s
V_z	hourly-mean wind speed at height z over the site	m/s	ft/s
V_{10}	V_z at z = 10 m over site	m/s	ft/s
x, y, z	system of rectangular cartesian co-ordinates with x-axis defined in direction of mean wind and z-axis vertical	m	ft
$\Delta x, \Delta y, \Delta z$	$x-x', y-y', z-z'$	m	ft
Δx_e	equivalent longitudinal separation equal to $x-x' + V_m\tau$	m	ft
z	effective height above ground level obstructions	m	ft
z_m	mean effective height; ½$(z+z')$	m	ft
z_0	surface roughness parameter of site	m	ft
$\gamma_{ii}^2\{r, r'; n\}$ $\gamma_{ii}^2\{\Delta r\}$	coherence function; $\lvert S_{ii}^2\{\Delta r\}\rvert/[S_{ii}\cdot S'_{ii}]$		
η	generalised non-dimensional separation parameter given by Equation (7.10) for isotropic turbulence (see footnote to Section 2.2)		
η_1	transformed value of η given by Equation (7.12) for non-isotropic turbulence		
$\theta_{ii}\{\Delta r\}; \theta_{ii}$	phase shift or lag angle (see Section 7.2)	rad	rad
$\rho_{ii}\{r, r'; \tau\}$, $\rho_{ii}\{\Delta r\}$	cross-correlation function; $C_{ii}\{\Delta r\}/(\sigma_i\sigma'_i)$		

$\rho_{ii}\{\Delta r;\ 0\}$	zero-lag cross-correlation function		
$\rho_{ii}\{\Delta r\}_{sym}$	symmetrical or even part of cross-correlation function		
$\rho_{ii}\{\Delta r\}_{antisym}$	anti-symmetrical part of cross-correlation function		
σ_i	standard deviation of *u*-, *v*- or *w*- component for averaging time $\to 0$ over period $\to 1$hr	m/s	ft/s
τ	incremental time lag	s	s
$\phi_{ii}\{\Delta r\};\ \phi_{ii}$	eddy slope, $\theta_{ii}\{\Delta r\}/(2\pi n\Delta r/V_m)$	rad	rad

Suffixes

i, *j*	refer to *u*-, *v*- or *w*- component
r	refers to direction of separation between points *r* and *r*'

A prime (') denotes a value at the point *r*' or (*x*', *y*', *z*').

2. BACKGROUND AND SUMMARY OF DATA PRESENTED

2.1 Purpose and Applicability

The fluctuating wind may be considered to be composed of a mean value on which is superimposed turbulence comprising fluctuating gust velocities in different directions. The properties of the mean wind speed (variation with height, surface roughness and averaging time) are dealt with in Items 82026, 84011 and 83045. The definitions of the statistical terms used to describe the properties of atmospheric turbulence and other background information are given in Item 74030[1] . Data giving the properties of turbulence in the atmospheric boundary layer measured at single points in space (probability densities, variances, autocorrelation and spectral density functions) are given in Item 85020[3] .

The purpose of this Item is to provide a means of determining the statistical properties describing the relation between the same gust components (*u*, *v* or *w*) measured at different points in space. Data are presented for heights throughout the atmospheric boundary layer for strong winds ($V_{10} \geq 10$ m/s) or neutral atmosphere conditions.

The main application is to structures (either aircraft or ground-based) of sufficient size that the non-uniform variation of gusts acting at different points causes a reduction in the maximum fluctuating loading. This is due to the incomplete correlation of gust properties over the structure at a particular instant or at a particular frequency. The same effect may also induce a significant fluctuating torque even when the mean torque is zero. Procedures using these data for estimating along-wind loading due to buffeting by turbulence are described in Item 76001 (Superseded by Items 87035 and 88019).

In general, the statistical quantities that describe these properties in the amplitude, time and frequency domains are:

(i) joint-probability densities,
(ii) cross-correlation functions,
(iii) cross-spectral densities or coherence functions.

The data presented in this Item describe the relation between the same gust components measured at different points in space. The cases considered include all three components (u, v and w) at points separated in the three principal directions (x, y, z) but guidance is given on extending the data to apply to points separated in any general direction.

2.2 Basis of the Data Presented

In general, reliable data for cross-correlations or coherence functions for strong winds (neutral atmosphere) are sparsely reported in the literature and many of these show considerable variations from each other due to

(i) inadequate data processing in some cases, particularly those data with trends,

(ii) non-standard conditions, *e.g.* non-neutral atmospheric stability and non-uniform terrain.

Because of this, the data presented in this Item are based on theoretical models, modified to take into account the deviations from the theory as obtained from those data that have been assessed to be the most reliable. In this way the effect of parameters such as terrain roughness, mean wind speed and height above the ground can be taken into account systematically. Additionally, extrapolation of the model to situations where no measured data are available can be made with more confidence, particularly for the high wind speeds appropriate to design conditions.

General expressions for the cross-correlation functions, derived from the modified von Karman model described in Item 85020, are given in Section 5. The corresponding Fourier transform of these relations, to provide cross-spectral density functions (or in normalised form, the coherence functions) cannot be obtained in convenient analytical form. Because of this a separate model is developed, again based on the theoretical von Karman equations for isotropic* turbulence but modified empirically to account for the significant departure from isotropy near the ground. This model is described in Section 7.

The theoretical equations on which the models are based are complicated expressions and for convenience they have been fitted with simpler expressions with little loss in accuracy.

Integral length scales of turbulence are required in estimating both cross-correlation and coherence data and equations for them are given in Section 6. These are based on measured data and are consistent with the concepts of similarity theory and theoretical relationships which enable length scales to be expressed in terms of the standard deviation (σ_i) and hourly-mean wind speed. In practice it is possible to relate all length scales to ${}^{x}L_u$ by simple expressions dependent on z/h.

2.2.1 Sources of data and uncertainty

The majority of available measurements (summarised in Table 2.1) are for relatively smooth terrains although some data for built-up areas are available in Derivations 6 and 16. Measurements at points with vertical separations are limited to heights below about 180 m and measurements with lateral separations are limited to heights below about 60 m. Furthermore there are comparatively few detailed measurements in strong winds (neutral atmosphere) and in particular it must be emphasised that no measurements are available for the high wind speeds associated with design conditions ($V_{10} > 20$ m/s). However, despite the limitations of the available data, the theoretical basis of the models adopted lends confidence in extrapolating to conditions that are different from those for which the applicability of the model has been confirmed. Thus, the data in this Item may be used for wind speeds up to design conditions, for heights up to at least 300 m and, tentatively, for surface roughnesses corresponding to $0.0001 \text{ m} \le z_0 \le 0.7 \text{ m}$.

* For isotropic turbulence the statistical properties do not change when the reference co-ordinate axes are rotated, *i.e.* the properties are independent of direction in the turbulence field. This only occurs in the layer above that containing the taller ground-based structures.

It is not possible to assess precisely the accuracy of the data presented in this Item although by taking ±25% on ${}^{r}L_{i}$ an estimate can be made of the uncertainty of the various functions that would be obtained under conditions of ideal processing and stationarity.

TABLE 2.1 Summary of Principal Data Considered

Derivation No. (see Section 8)	Velocity Components	Separation Δr	Height range of measurements (m)	Terrain
8	u; v	Δz	15 – 155	summary of several sources (open country, brush woods, desert brush)
9, 10, 16	u; w	Δy	20, 40	island; coastal waters and
	u	Δz	30 – 150	open country
12	u; v	Δy	3 – 18	short grass
12	u; v	Δz	17 – 182	open country
15, 17	u; v	Δy, Δz	10 – 60	wind from suburban terrain
18	u	Δz	1 – 8	wind from the sea
19	u; v; w	Δy	11	snow-covered rolling terrain
20	u	Δy	3; 57	ice; water
21	u; v; w	Δz	3 – 22	open country
21	u	Δy	10	open country

3. INPUT DATA

A description of the atmospheric boundary layer and the mechanisms producing turbulence is contained in Item No. 74030. The main factors that affect the production and properties of turbulence in the neutral atmospheric boundary layer (and hence the parameters that are required as input data when using this Item) are as follows.

(i) The hourly-mean wind speed at the site in question: the variation of mean wind speed with height and terrain roughness is dealt with in Items 82026 and 84011 and the user should refer to those documents for data appropriate to strong wind or neutral atmosphere conditions.

(ii) The longitudinal integral length scale of turbulence, ${}^{x}L_{u}$ (from which all other length scales can be determined) for the appropriate terrain, wind speed and heights above the ground over the site at which data are required: this can be obtained from Item 85020. **Note that due to their dependence on mean wind speed, length scales at design wind speeds (V_{10} = 20 to 35 m/s) are much larger than typical values reported in the literature which have been obtained at more moderate wind speeds (typically V_{10} = 10 m/s).** Note also that the effect on ${}^{x}L_{u}$ of any significant step changes in terrain roughness upwind of the site should be taken into account as described in Item 85020; this is particularly important when the site is in a built-up area.

(iii) The atmospheric boundary layer depth, h: for the purposes of using this Data Item it is a sufficient approximation to use $h = (1/6)\ u_{*} \times 10^{4}$ where u_{*} is the friction velocity given by $u_{*} = V_{10}/(2.5 \ln (10/z_{0}))$. Note that with V_{10} and z_{0} in m/s and m respectively, the unit of h is metres.

To determine the cross-covariance ($C_{ii}\{\Delta r\}$) or cross-spectral density ($S_{ii}\{\Delta r\}$) from data given in this Item, values of S_{ii} and σ_i are required. These can be obtained from Item 85020 for appropriate values of V_z, z and z_0. For cases where the separation between points is not in the vertical direction (*i.e.* $z = z'$), it may be assumed that $S_{ii} = S'_{ii}$ and $\sigma_i = \sigma_i'$.

4. JOINT-PROBABILITY DENSITY

The probability of the occurrence of a single event or quantity, or the probability density distribution of a single fluctuating quantity (such as u) is described in Items 74030 and 85020. However, it is sometimes necessary to consider the combined probability $P\{i,j\}$ that particular values (i_p and j_p) of two components $i\{r\}$ and $j\{r'\}$ will occur together.

When these quantities are entirely unrelated, the combined probability is simply the product of the probabilities of the two separate events. For example, the joint probability of throwing a (1) followed by a (2) in successive throws of a conventional six-sided dice is $P(1, 2) = P(1).\ P(2) = (1/6) \times (1/6) = 1/36$.

When these quantities are completely correlated then the joint and the individual probabilities are equal.

In practice these quantities are usually partly related and the joint probability lies between these two limiting cases. It is thus not only a function of the individual probability densities $p(i)$ and $p(j)$ but depends in a more general way on i and j. The joint probability $P\{i,j\}$ that the two fluctuating quantities $i\{r\}$ and $j\{r'\}$ will be less than i_p and j_p respectively is related to the joint-probability density function in a way analogous to that for a single variable (see Items 74030 and 85020), *i.e.*

$$P\{i,j\} = \int_{-\infty}^{j_p} \int_{-\infty}^{i_p} p\{i,j\}\,\mathrm{d}i\ \mathrm{d}j \tag{4.1}$$

where

$$\int_{-\infty}^{\infty} \int_{-\infty}^{\infty} p\{i,j\}\,\mathrm{d}i\ \mathrm{d}j = 1\,. \tag{4.2}$$

Very few joint-probability density measurements of related gust components in the atmosphere have been made. In the absence of more specific information a Gaussian, or normal, joint-probability density function may be assumed which, for two fluctuating quantities i and j (here $i = u$, v or w), is given by

$$p\{i,j\} = \frac{1}{2\pi\sigma_i\sigma_j[1-\rho_{ij}^2]^{1/2}} \exp -\left[\frac{i^2\sigma_j^2 - 2ij\sigma_i\sigma_j\rho_{ij} + j^2\sigma_i^2}{2\sigma_i^2\sigma_j^2[1-\rho_{ij}^2]}\right] \tag{4.3}$$

where ρ_{ij} is the corresponding cross-correlation function (see Section 5.1).

5. CROSS-CORRELATION FUNCTIONS

The cross-correlation functions characterise the relationship between fluctuating velocity components at 2 points in space (separated by Δr) and in the general case at different times (time lag τ). The zero-lag ($\tau = 0$) cross-correlations are especially important since they describe how the instantaneous fluctuating component of wind velocity varies in space. This forms the basis of calculating the maximum fluctuating wind-loading component when dynamic effects due to oscillation of the structure can be ignored.

Because changes in the gust velocity at one point (r) are not necessarily reflected immediately by similar changes in the gust velocity at another point (r'), the cross-correlation functions are not, in general,

symmetrical functions of τ about the $\tau = 0$ axis. For example, changes in u at height z and time t are followed by related changes in u at a lower height z' at some time $t+\tau$ later. However, as shown in Item No. 74030, the cross-correlation function can be considered to be composed of two components, the larger one being a symmetrical function of τ and the other being an anti-symmetrical function of τ (see Sketch 5.1). These are Fourier transforms of the real (co-spectral density) and imaginary (quad-spectral density*) parts respectively of the cross-spectral density function (see Section 7). Thus the cross-correlation function can be written as

$$\rho_{ii}\{\Delta r\} = \rho_{ii}\{\Delta r\}_{sym} + \rho_{ii}\{\Delta r\}_{antisym} \tag{5.1}$$

where
$$\rho_{ii}\{\Delta r\}_{sym} = \frac{1}{\sigma_i \sigma_i'} \int_0^\infty P\ \{\Delta r\} \cos(2\pi n\tau) \mathrm{d}n \tag{5.2}$$

and
$$\rho_{ii}\{\Delta r\}_{antisym} = \frac{1}{\sigma_i \sigma_i'} \int_0^\infty Q\ \{\Delta r\} \sin(2\pi n\tau) \mathrm{d}n\,. \tag{5.3}$$

However, more convenient expressions for the zero-lag and symmetrical parts of the cross-correlation functions are given in Section 5.1.

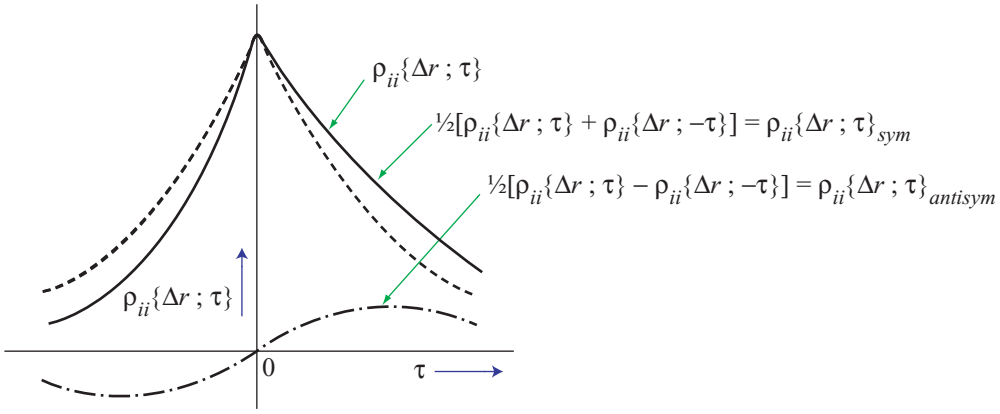

Sketch 5.1 Illustration of symmetrical and anti-symmetrical parts of cross-correlation function

5.1 Analytical Expressions for the Cross-correlation Functions

The zero-lag ($\tau = 0$) cross-correlations, and the even or symmetrical part of the cross-correlation function for $\tau = 0$, can be obtained in terms of the basic longitudinal and lateral autocorrelation functions (f and g) given in Item 85020†. Assuming that a time lag τ can be converted to an equivalent spatial separation equal to $V_z\,\tau$ (Taylor's hypothesis) the symmetrical part of the cross-correlation function can be estimated from the modified equations for isotropic turbulence with appropriate values of the length scale to allow for the distortion of turbulence close to the ground. In general terms Equation (5.4) applies when $i = u$, v or w and is valid for separations between two points in any direction with or without a time lag τ. The important zero-lag cross-correlation cases are summarised in Section 5.1.1 since these functions are of

* The quad-spectral density function is usually small and so is often ignored (see Section 7.2). It follows that the anti-symmetrical part of $\rho_{ii}\{\Delta r\}$ is also small and negligible. Furthermore, when used, for example, in calculating the fluctuating component of wind loading due to turbulence the antisymmetric and quad-coherence components integrate to zero over the structure.

† The autocorrelation functions in Item 85020 are derived from the von Karman equations for isotropic turbulence with modifications to account for observed departures from the theory close to the ground.

particular importance when evaluating fluctuating wind loads on structures.

$$\rho_{ii}\,\{\Delta r\}_{sym} = \frac{f-g}{\Delta r_e^2}\,\Delta s_i^2 + g\,. \tag{5.4}$$

The longitudinal and lateral correlation functions (f and g respectively) can be evaluated from Figure 1, taken from Item 85020. The parameters Δs_i and Δr_e are equated respectively to the longitudinal and lateral separations with respect to the axis along which the component (u, v or w) acts and these are summarised in Table 5.1 and also on Figure 1.

As can be seen from Figure 1, and noted in Item 85020, the dependence on z/h is small. To a sufficiently close approximation the f and g functions can be represented by the following equations, independent of z/h.

$$f = \tfrac{1}{2}\,(f_1 + f_1^{\,2}) \tag{5.5}$$

$$g = \tfrac{1}{2}\,(g_1 + g_1^{\,2}) \tag{5.6}$$

where
$$f_1 = \exp[-0.822(\tilde{r}_f)^{0.77}] \tag{5.7}$$

$$g_1 = \exp[-1.23(\tilde{r}_g)^{0.85}] \tag{5.8}$$

where $\tilde{r}_f = \Delta r_i / {}^{r}L_i$ and $\tilde{r}_g = \Delta r_i / (2\,{}^{r}L_i)$.

The length scale parameter, ${}^{r}L_i$, depends on the gust components ($i = u$, v or w) under consideration and the direction in space of the spatial separation. In evaluating the f-function, ${}^{r}L_i$ is taken as the longitudinal length scale ${}^{x}L_u$, ${}^{y}L_v$ or ${}^{z}L_w$ for the u-, v- or w- component respectively. For the g-function a compound lateral length scale is used based on weighted contributions from each lateral separation normal to the axis along which the particular gust component acts. For convenience these parameters are summarised in Table 5.1 and equations for each length scale are given in Section 6.

TABLE 5.1 Summary Chart for Cross-Correlation Functions (Equation (5.4))

Component	u	v	w
Δr^2	$= \Delta x^2 + \Delta y^2 + \Delta z^2$		
Δs_i^2	$(\tau V_m + \Delta x)^2$	Δy^2	Δz^2
Δr_e^2	$= (\tau V_m + \Delta x)^2 + \Delta y^2 + \Delta z^2$		
f-function Δr_i	$= \Delta s_i$	$= \Delta s_i$	$= \Delta s_i$
${}^{r}L_i$	${}^{x}L_u$	${}^{y}L_v$	${}^{z}L_w$
g-function Δr_i	$= (\Delta r_e^{\,2} - \Delta s_i^{\,2})^{1/2}$		
${}^{r}L_i$	see Equation (6.15)	see Equation (6.16)	see Equation (6.17)

5.1.1 Zero-lag cross-correlations

The zero-lag cross-correlations are of particular interest and those of more practical importance are given by Equation (5.4), or Figure 1, as follows

$$\rho_{uu}\{\Delta y;0\} = g \text{ with } \tilde{r}_g = \Delta y /(2^{y}L_u) \tag{5.9}$$

$$\rho_{uu}\{\Delta z;0\} = g \text{ with } \tilde{r}_g = \Delta z /(2^{z}L_u) \tag{5.10}$$

$$\rho_{uu}\{\Delta r;0\} = g \text{ with } \tilde{r}_g = \Delta r /(2^{r}L_u);\ \Delta r = (\Delta y^2 + \Delta z^2)^{1/2} \tag{5.11}$$

$$\rho_{vv}\{\Delta z;0\} = g \text{ with } \tilde{r}_g = \Delta z /(2^{z}L_v) \tag{5.12}$$

$$\rho_{ww}\{\Delta y;0\} = g \text{ with } \tilde{r}_g = \Delta y /(2^{y}L_w)\,. \tag{5.13}$$

6. LENGTH SCALES OF TURBULENCE

The length scales of turbulence are a comparative measure of the "average size" of a gust in appropriate directions and are important scaling factors in determining how rapidly gust properties vary in space. For example, ${}^{y}L_u$ is a length scale of the u gust component measured in the y direction. In practice it is usually defined as an integral length scale since it is determined from an integration, with respect to separation distance, of the appropriate zero-lag cross-correlation function. Thus,

$${}^{y}L_u = \int_0^\infty \rho_{uu}\{\Delta y;\ 0\}\,\mathrm{d}(\Delta y)$$

where $\rho_{uu}\{\Delta y;\ 0\}$ is the cross-correlation function for zero lag between u gust components measured at points separated in the y direction. The length scales ${}^{x}L_u$, ${}^{y}L_v$ and ${}^{z}L_w$ are called longitudinal length scales because the direction of the gust components being correlated at two points is parallel to the line joining the two points. Conversely, the length scales ${}^{y}L_u$, ${}^{z}L_u$, ${}^{x}L_v$, ${}^{z}L_v$, ${}^{x}L_w$ and ${}^{y}L_w$ are called lateral length scales. The length scales increase with increasing height above the ground up to an asymptotic value at the edge of the atmospheric boundary layer (gradient height). Also, for a given height, they increase with increasing wind speed and surface roughness. The reason for this is that as wind strength increases the boundary layer height increases and eddies within the boundary layer are stretched accordingly.

At the upper edge of the boundary layer, for a given wind speed and surface roughness, all the longitudinal length scales tend to the same value which is equal to twice* the value of the lateral scales. This is why, when lateral separations and length scales are involved, the non-dimensional separation parameter (relating separation distance to typical eddy size) appears in the form $\Delta r/(2^{r}L_i)$. In reality, the ratio between the longitudinal and lateral length scales is 2 only in the upper part of the boundary layer; at lower heights this ratio increases and is different for each component.

* The factor of '2' derives from the condition for flow continuity which imposes the relationship $g = f + \tfrac{1}{2}\,\tilde{r}\,\mathrm{d}f/\mathrm{d}\tilde{r}$ which gives the result that $\int_0^\infty f\,\mathrm{d}\tilde{r} = 2\int_0^\infty g\,\mathrm{d}\tilde{r}$.

6.1 Principal Length Scales

As explained in Section A1.2 of the Appendix, because of the existence of isotropy in the high frequency region it follows that, theoretically, the following relations exist between the various length scales, and these are found to be justified in practice,

$$\frac{2^{x}L_v}{{}^{x}L_u} = \left(\frac{\sigma_v}{\sigma_u}\right)^3 = \frac{{}^{y}L_v}{2^{y}L_u} = \frac{2^{z}L_v}{2^{z}L_u} \tag{6.1}$$

$$\frac{2^{x}L_w}{{}^{x}L_u} = \left(\frac{\sigma_w}{\sigma_u}\right)^3 = \frac{2^{y}L_w}{2^{y}L_u} = \frac{{}^{z}L_w}{2^{z}L_u}\,. \tag{6.2}$$

Furthermore, the length scales ${}^{y}L_u$ and ${}^{z}L_u$ are found, from analyses of measurements in the atmospheric boundary layer, to be related to ${}^{x}L_u$ by

$$\frac{{}^{z}L_u}{{}^{x}L_u} = 0.5 - 0.34\exp[-35(z/h)^{1.7}] \tag{6.3}$$

$$\frac{{}^{y}L_u}{{}^{x}L_u} = 0.16 + 0.68\,{}^{z}L_u/{}^{x}L_u\,. \tag{6.4}$$

Given ${}^{x}L_u$ (which can be obtained from Item 85020 for uniform or non-uniform terrain), Equations (6.1) to (6.4) then define all the remaining principal length scales using relations for σ_v/σ_u and σ_w/σ_u from ESDU 85020 which are

$$\sigma_v/\sigma_u = 1 - 0.22\cos^4\left(\frac{\pi z}{2h}\right) \tag{6.5}$$

$$\sigma_w/\sigma_u = 1 - 0.45\cos^4\left(\frac{\pi z}{2h}\right)\,. \tag{6.6}$$

The principal length scales are then given by

$$2^{y}L_u / {}^{x}L_u = 1.0 - 0.46\exp[-35(z/h)^{1.7}] \tag{6.7}$$

$$2^{z}L_u / {}^{x}L_u = 1.0 - 0.68\exp[-35(z/h)^{1.7}] \tag{6.8}$$

$$2^{x}L_v / {}^{x}L_u = (\sigma_v/\sigma_u)^3 \tag{6.9}$$

$${}^{y}L_v / {}^{x}L_u = (2^{y}L_u / {}^{x}L_u)(\sigma_v/\sigma_u)^3 \tag{6.10}$$

$$2^{z}L_v / {}^{x}L_u = (2^{z}L_u / {}^{x}L_u)(\sigma_v/\sigma_u)^3 \tag{6.11}$$

$$2^{x}L_w / {}^{x}L_u = (\sigma_w/\sigma_u)^3 \tag{6.12}$$

$$2^{y}L_w / {}^{x}L_u = (2^{y}L_u / {}^{x}L_u)(\sigma_w/\sigma_u)^3 \tag{6.13}$$

$${}^{z}L_w / {}^{x}L_u = (2^{z}L_u / {}^{x}L_u)(\sigma_w/\sigma_u)^3\,. \tag{6.14}$$

6.2 Compound Length Scales

When the spatial separations between points at which the various turbulence properties are being considered are not in a direction along one of the principal axes (x, y or z), as illustrated in Sketch 6.1, then compound length scales must be used. It is recommended that these be estimated using Equations (6.15) to (6.17) which provide compounded mean values of the appropriate principal length scales weighted in accordance with the component separation distances resolved along the principal axes.

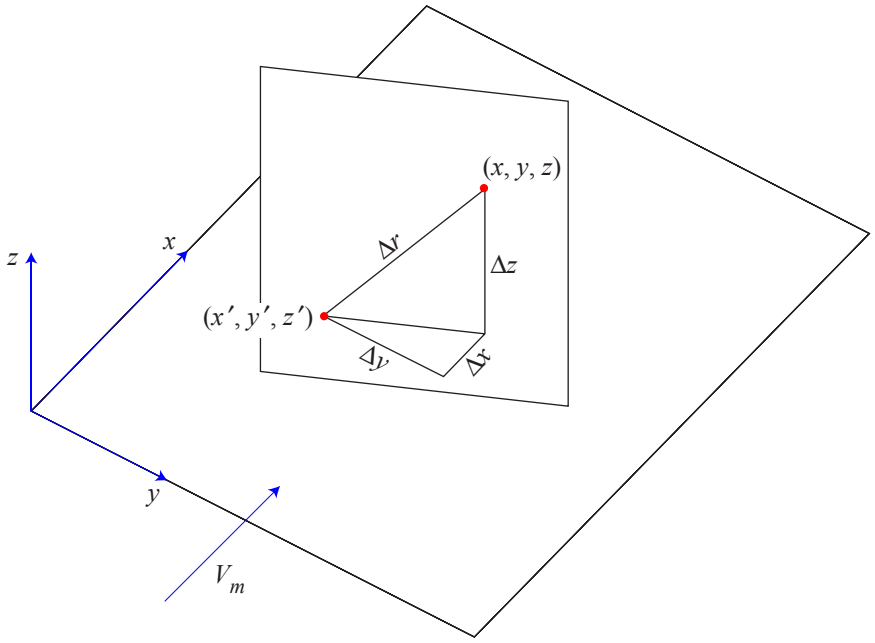

Sketch 6.1

For u components with lateral and vertical separations, the length scale is

$$ {}^{r}L_u = \frac{\left[\left({}^{y}L_u \cdot \Delta y \right)^2 + \left({}^{z}L_u \cdot \Delta z \right)^2 \right]^{1/2}}{\left(\Delta y^2 + \Delta z^2 \right)^{1/2}} \quad . \tag{6.15} $$

Similarly, for v components with longitudinal and vertical separations

$$ {}^{r}L_v = \frac{\left[\left({}^{x}L_v \cdot \Delta x \right)^2 + \left({}^{z}L_v \cdot \Delta z \right)^2 \right]^{1/2}}{\left(\Delta x^2 + \Delta z^2 \right)^{1/2}} \tag{6.16} $$

and for w components with longitudinal and lateral separations

$$ {}^{r}L_w = \frac{\left[\left({}^{x}L_w \cdot \Delta x \right)^2 + \left({}^{y}L_w \cdot \Delta y \right)^2 \right]^{1/2}}{\left(\Delta x^2 + \Delta y^2 \right)^{1/2}} \quad . \tag{6.17} $$

7. CROSS-SPECTRAL DENSITY AND COHERENCE FUNCTIONS

The frequency-dependent coherence functions gives a relative measure of how the energy in a gust of a particular frequency varies in space between one point and another. In effect these behave, for a particular frequency, in a manner similar to zero-lag cross-correlation functions. The coherence function (which varies with n and Δr) is formed by normalising the square of the cross-spectral density between two points (r and r') with respect to the product of the spectral densities at each point. Thus as Δr increases from zero the coherence falls from unity and tends to zero.

The cross-spectral density function in its general form is a complex quantity which can be expressed as a modulus and phase angle or as the sum of real (in-phase) and imaginary (out-of-phase) components, *i.e.* (noting that $\hat{\imath} = \sqrt{-1}$)

$$S_{ii}\{r, r';n\} = S_{ii}\{\Delta r\} = \left|S_{ii}\{\Delta r\}\right|\exp(-\hat{\imath}\theta)$$
$$= \left|S_{ii}\{\Delta r\}\right|\cos(\theta_{ii} - \hat{\imath}\,\sin\theta_{ii}) = P_{ii}\{\Delta r\} - \hat{\imath}Q_{ii}\{\Delta r\}\ . \qquad (7.1)$$

The functions $P_{ii}\{\Delta r\}$ and $Q_{ii}\{\Delta r\}$ are called the co-spectral density and quad-spectral density functions respectively and are related by the phase-lag angle given by

$$\theta_{ii}\{\Delta r\} = \tan^{-1}\frac{Q_{ii}\{\Delta r\}}{P_{ii}\{\Delta r\}}\ . \qquad (7.2)$$

The phase angle is sometimes expressed in terms of an "eddy slope" defined as

$$\phi_{ii}\{\Delta r\} = \frac{\theta_{ii}\{\Delta r\}}{2\pi n\Delta r/V_m}\ . \qquad (7.3)$$

The normalised form of the cross-spectral function, called the coherence function, $\gamma^2_{ii}\{\Delta r\}$, is often used and is defined as

$$\gamma^2_{ii}\{\Delta r\} = \frac{\left|S_{ii}\{\Delta r\}\right|^2}{S_{ii}\,.\,S'_{ii}} = \frac{P^2_{ii}\{\Delta r\} + Q^2_{ii}\{\Delta r\}}{S_{ii}\,.\,S'_{ii}} \qquad (7.4)$$

where S_{ii} and S'_{ii} are the single point spectral density functions at the two points r and r' and the quantities $P^2_{ii}\{\Delta r\}/[S_{ii}\cdot S'_{ii}]$ and $Q^2_{ii}(\{\Delta r\}/[S_{ii}\cdot S'_{ii}])$ are often called the co-coherence and quad-coherence functions respectively.

It should be remembered that in calculating the fluctuating loading component due to gusts acting on a structure the summation of contributions from all pairs of points (r and r') on the structure only involves the co-coherence function since the out-of-phase component (the quad-coherence) integrates to zero.

For most cases when $\Delta r = \Delta y$ or Δz, $\left|Q_{ii}\{\Delta r\}\right|$ is small so that for most applications the quad-coherence can be assumed zero and the coherence then equals the co-coherence. The quad-spectral density, $Q_{vv}\{\Delta z\}$, is larger than the other values but even this is only significant near the ground and in this case Section 7.2 should be consulted.

Means of evaluating values of $P_{ii}\{\Delta r\}$ and $Q_{ii}\{\Delta r\}$ for the specific cases when the mean wind direction is parallel or normal to the line joining the points under consideration are given in Section 7.2. These data are summarised in Table 7.1 which also gives suggestions for extending the data to non-standard cases (*e.g.*

when the direction of the spatial separation is not along one of the principal axes).

7.1 Coherence Functions

The best fit to measured data is obtained using equations which are a simplified approximation to the von Karman spectral equations modified to account for the departure from isotropic conditions near the ground. Section A2 in Appendix A describes the derivation of these equations which are summarised in Section 7.1.2.

In most sources of data the root-coherence function is approximated by a simple exponential expression of the form

$$\sqrt{\text{coherence}} = \gamma_{ii}\{\Delta r\} = \exp(-a_{ii} n\ \Delta r/V_m)\ ,\ (i = u,\ v,\ w;\ r = y,\ z) \tag{7.5}$$

where the value of the decay constant a_{ii} is varied empirically according to the component and direction of separation.

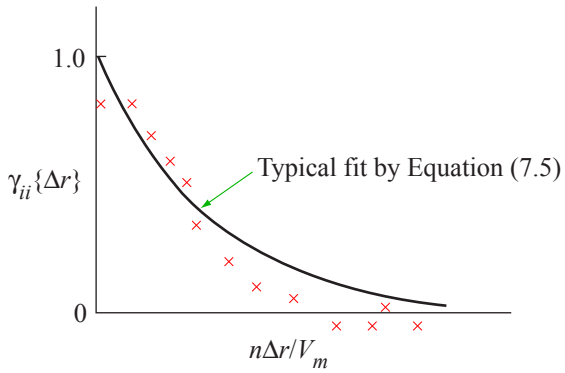

Sketch 7.1

This form of expression has limitations in fitting measured data over the whole frequency range as illustrated in Sketch 7.1. In particular the trend to $\gamma_{ii} = 1.0$ as $n\ \Delta r/V_m \to 0$ is incorrect since, even as n decreases and eddies become larger, measurements between two points separated in space will never be completely coherent. Significant errors are introduced, especially for the v- and w-components, as $n \to 0$ particularly when $\Delta r/(2\ ^{r}L_i)$ is large. Furthermore, the extrapolation of this equation, fitted to data for moderate wind speeds, will tend to overestimate γ_{ii} when used for much higher design wind speeds.

Values of the parameter a_{ii} in Equation (7.5) may be derived for specific values of $n\ \Delta r/V_m$ from the more appropriate equation in Section 7.1.2. The derivation of expressions for a_{ii} is given in Section A2.1 of the Appendix where comparison is made with data correlations from other sources that have used Equation (7.5) to fit measured coherence data.

7.1.1 Separations in along-wind direction

When the direction of the spatial separations is in the along-wind direction (*i.e.* $\Delta r = \Delta x$) then, on the assumption that Taylor's hypothesis of "frozen turbulence" applies, Δx can be converted to an equivalent time lag of $\Delta x/V_z$. The problem then reduces to that associated with time or frequency variations at a single point together with a phase angle to account for the phase lag between the upstream and downstream fluctuating velocity signals which, by Taylor's hypothesis, are otherwise identical. Thus, in this case the coherence function would be unity and $\theta = 2\pi n\Delta x/V_z$. In practice, Taylor's hypothesis is not always

strictly applicable (particularly near the ground and when V_z/n is greater than about 300 m) and the coherence function is generally less than unity. However, few measured data for a neutral atmosphere have been found to quantify this reduction but Derivations 13 and 14 indicate that a reasonable assumption is

$$\sqrt{\text{coherence}} = \gamma_{ii}\{\Delta x\} \approx \exp(-a_{ii} n\, \Delta x/V_z) \tag{7.6}$$

with $a_{uu} \approx 3$ and $a_{vv} \approx 6$.

7.1.2 Separations normal to wind direction

For u components with separations in the lateral $(\Delta r = \Delta y)$ or vertical $(\Delta r = \Delta z)$ directions the root-coherence function (based on a modified form of the von Karman spectral equations, see Section A2 of Appendix A) is given by

$$\sqrt{\text{coherence}} = \gamma_{uu}\{\Delta r\} = \exp(-1.15\eta_1^{1.5}) \tag{7.7}$$

when η_1 is determined from the following sequential calculations,

$$\tilde{r}_g = \Delta r/(2\,{}^{r}L_u) \text{ where } {}^{r}L_u \text{ is taken at the mean height} \tag{7.8}$$

$$b = 0.35\tilde{r}_g^{\,0.2} \tag{7.9}$$

$$\eta = [(0.747\tilde{r}_g)^2 + (2\pi n \Delta r/V_m)^2]^{1/2} \tag{7.10}$$

$$c = \frac{1.6\tilde{r}_g^{\,0.13}}{\eta^b} \text{ or 1.0, whichever is greater} \tag{7.11}$$

$$\eta_1 = [(0.747\tilde{r}_g)^2 + (c2\pi n \Delta r/V_m)^2]^{1/2}. \tag{7.12}$$

Note that for the high frequency region, which is of most interest in calculating dynamic effects for practical structures, the expression for η_1 simplifies to

$$\eta_1 = c(2\pi n \Delta r/V_m). \tag{7.13}$$

For the u-component the length scale parameter, ${}^{r}L_i$, is defined as

$${}^{r}L_i = {}^{y}L_u \text{ for lateral separation } \Delta y,$$

$${}^{r}L_i = {}^{z}L_u \text{ for vertical separation } \Delta z,$$

$${}^{r}L_i = \frac{\left[({}^{y}L_u \Delta y)^2 + ({}^{z}L_u \Delta z)^2\right]^{1/2}}{\Delta r} \text{ for separation } \Delta r = (\Delta y^2 + \Delta z^2)^{1/2}.$$

For the v- and w- components the corresponding equations (based on the modified von Karman model, see Section A2 of Appendix A) are

$$\sqrt{\text{coherence}} = \gamma_{vv}\{\Delta r\} = \exp(-0.65\eta_1^{1.3}) \tag{7.14}$$

where η_1 is given by Equations (7.8) to (7.12) with ${}^{r}L_u$ replaced by ${}^{r}L_v$ or ${}^{r}L_w$ for the *v*- and *w*-components respectively as summarised in Table 7.1.

7.2 Co-coherence, Quad-coherence Functions; Phase Angle

The co-spectral and quad-spectral density components can be obtained from the cross-spectral density using Equation (7.1) with known values of the phase angle. The root co-coherence and root quad-coherence are then given respectively by

$$\frac{P_{ii}\{\Delta r\}}{(S_{ii} \,.\, S'_{ii})^{\frac{1}{2}}} = \gamma_{ii}\{\Delta r\} \cos \theta_{ii}, \tag{7.15}$$

$$\frac{Q_{ii}\{\Delta r\}}{(S_{ii} \,.\, S'_{ii})^{\frac{1}{2}}} = \gamma_{ii}\{\Delta r\} \sin \theta_{ii}. \tag{7.16}$$

When θ_{ii} is greater than zero it implies that changes in the fluctuating velocity component at the point *r* are followed by similar changes at the point *r*' at some time later. In practice the phase angle varies erratically but its effect on the cross-spectrum is generally small and is ignored except in the case of $\theta_{vv}\{\Delta z\}$ which makes the corresponding root co-coherence significantly different from $\gamma_{vv}\{\Delta z\}$.

7.2.1 Phase angle for horizontal separations

For separations in the lateral *y*-direction θ_{ii} can be taken as zero.

For separations in the mean wind direction, assuming that Δx can be converted to an equivalent time lag $\Delta x/V_z$ (Taylor's hypothesis), the phase angle is $2\pi n\Delta x/V_z$ (and $\phi_{ii} = 1$).

7.2.2 Phase angle for vertical separations

For separations in the vertical direction the eddies are inclined with the mean wind shear so that changes in the gust component higher up are followed by similar changes lower down at some time later. Thus, in general, $\theta_{uu}\{\Delta z\}$ and $\theta_{vv}\{\Delta z\}$ are not zero although they must tend to zero as *z* increases and $\mathrm{d}V_z/\mathrm{d}z$ tends to zero.

Thus, for isotropic turbulence the phase difference between gust velocities separated vertically is zero, no matter what the value of Δz and *z*. This also applies to the high frequency range when, even near the ground, turbulence exhibits isotropic properties.

Based on an empirical correlation of data[21] at low frequencies from a number of different sources up to about 80 m, the eddy slope ϕ_{ii} is approximately 1.3 $\Delta z/z_m$ for the *u*-component and 3 $\Delta z/z_m$ for the *v*-component. However, at higher frequencies it has been argued that since the properties of turbulence regain isotropic characteristics then θ_{ii} should tend to zero as *n* increases. Based on data for Rugby (z_0 = 0.03 m) and Cranfield (z_0 = 0.003 m) empirical relations which satisfy these conditions are

$$\theta_{uu}\{\Delta z\} = (1.3\ \Delta z/z_m)(c-1)^{0.7}\ (2\pi\ n\Delta z/V_m) \tag{7.17}$$

and

$$\theta_{vv}\{\Delta z\} = (3\ \Delta z/z_m)(c-1)^{0.7}\ (2\pi\ n\Delta z/V_m) \tag{7.18}$$

where c is derived from Equations (7.8) to (7.11) and in practice varies from a value of approximately 2 at low frequency to 1.0 at high frequencies.

For the u-component, $\theta_{uu}\{\Delta z\}$ is sufficiently small that the co-coherence can be equated to the coherence. This is not so for the v-component and $P_{vv}\{\Delta z\}$ is given by Equation (7.15).

For the w-component with vertical separations, no reliable data are available although this case is not of practical importance. However, Bowen *et al*.[21] report that for measurements over open country up to about 20 m, $\theta_{ww}\{\Delta z\} \approx 0$.

TABLE 7.1 Summary Chart for Coherence Functions

Gust components	Separation distance	$\sqrt{\text{Coherence}}$ (Section 7.1)	Phase angle, θ_{ii} (Sections 7.2.1, 7.2.2)	Δr in definition of η	${}^{r}L_i$
$u-u$	Δx	Eqn (7.6)	$2\pi n\ \Delta x/V_m$	–	–
$u-u$	Δy	Eqn (7.7)	0	Δy	Eqn (6.7)
$u-u$	Δz	Eqn (7.7)	Eqn (7.16)	Δz	Eqn (6.8)
$u-u$	$\sqrt{\Delta x^2+\Delta y^2}$	Eqn (7.7)	$2\pi n\ \Delta x/V_m$	Δy	Eqn (6.7)
$u-u$	$\sqrt{\Delta y^2+\Delta z^2}$	Eqn (7.7)	Eqn (7.16)	$\sqrt{\Delta y^2+\Delta z^2}$	Eqn (6.15)
$v-v$	Δx	Eqn (7.6)	$2\pi n\ \Delta x/V_m$	–	–
$v-v$	Δz	Eqn (7.14)	Eqn (7.17)	Δz	Eqn (6.11)
$w-w$	Δy	Eqn (7.14)	0	Δy	Eqn (6.13)
$w-w$	$\sqrt{\Delta x^2+\Delta y^2}$	Eqn (7.14)	$2\pi n\ \Delta x/V_m$	Δy	Eqn (6.13)

$$\sqrt{\text{Co-coherence}} = \gamma_{ii}\{\Delta r\}\ \cos\ \theta_{ii}$$

$$\sqrt{\text{Quad-coherence}} = \gamma_{ii}\{\Delta r\}\ \sin\ \theta_{ii}$$

8. REFERENCES AND DERIVATION

The references given are recommended sources of information supplementary to that in this Data Item.

References

1. ESDU — Characteristics of atmospheric turbulence near the ground. Part 1: definitions and general information. Item No. 74030, ESDU International, London, 1974.
2. ESDU — Strong winds in the atmospheric boundary layer. Part 1: mean-hourly wind speeds. Item No. 82026, ESDU International, London, 1982.
3. ESDU — Characteristics of atmospheric turbulence near the ground. Part II: single point data for strong winds (neutral atmosphere). Item No. 85020, ESDU International, London, 1985.

Derivation

The Derivation lists selected sources that have assisted in the preparation of this Data Item.

4. DAVENPORT, A.G. — The spectrum of horizontal gustiness near the ground in high winds. *Q. J. R. Met. Soc*., Vol. 87, pp. 194-211, April 1961.
5. PANOFSKY, H.A. SINGER, I.A. — Vertical structure of turbulence. *Q. J. R. Met. Soc*., Vol. 91, pp. 339-344, July 1965.
6. DAVENPORT, A.G. — The dependence of wind loads on meteorological parameters. Paper No. 2, Proc. Int. Res. Seminar "Wind effects on buildings and structures", Ottawa, Canada, Univ. Toronto Press, 1967.
7. HARRIS, R.I. — The nature of the wind. Paper No.5, Proc. CIRIA Seminar on "The modern design of wind-sensitive structures". Construction Industry Research and Information Association, London, June 1970.
8. PIELKE, R.A. PANOFSKY, H.A. — Turbulence characteristics along several towers. *Boundary-layer Met.*, Vol. 1, pp. 115-130, November 1970.
9. SHIOTANI, M. — Structures of gusts in high winds. Nihon University, Japan, Physical Sci. Lab. Interim Report, Parts 2-5, 1968-1971.
10. SHIOTANI, M. IWATANI, Y. — Correlations of wind velocities in relation to the gust loadings. Paper No. 6, Proc. Third Int. Conf. on "Wind effects on buildings and structures", Tokyo, Japan, 1971.
11. HARRIS, R.I. — Measurements of wind structure. Symposium on external flows, Bristol University, England, June 1972.
12. HARRIS, R.I. — Unpublished data, Cranfield Institute of Technology, England, 1972.
13. ROPELEWSKI, C.F. TENNEKES, H. PANOFSKY, H.A. — Horizontal coherence of wind fluctuations. *Boundary-layer Met.*, Vol. 5, pp. 353-363, July 1973.
14. POWELL, D.C. ELDERKIN, C.E. — An investigation of the application of Taylor's hypothesis to atmospheric boundary-layer turbulence. *J. Atmos. Sci.*, Vol. 31, pp. 990-1002, May 1974.

15. DUCHENE-MARULLAZ, P. — Turbulence atmospherique au voisinage d'une ville. Centre Scientifique et Technique du Batiment, Nantes, France, Rep. E.N. CL1 75-2, 1975.

16. SHIOTANI, M. IWATANI, Y. KUROHA, K. — Magnitudes and horizontal correlations of vertical velocities in high winds. *J. Met. Soc. Japan*, Vol. 56, No.1, pp. 35-42, February 1978.

17. DUCHENE-MARULLAZ, P. — Effect of high roughness on the characteristics of turbulence in cases of strong winds. Proc. 5th Int. Conf. on Wind Engng., Fort Collins, Colorado, USA, pp. 179-193, 1979.

18. STEGEN, G.R. THORPE, R.L. — Vertical coherence in the atmospheric boundary layer. Proc 5th Int. Conf. on Wind Engng, Fort Collins, Colorado, USA, pp. 203-214, 1979.

19. TEUNISSEN, H.W. — Structure of mean winds and turbulence in the planetary boundary layer over rural terrain. *Boundary-layer Met.*, Vol. 19, pp. 187-221, 1980.

20. KRISTENSEN, L. PANOFSKY, H.A. SMITH, S.D. — Lateral coherence of longitudinal wind components in strong winds. *Boundary-layer Met.*, Vol. 21, pp. 199-205, 1981.

21. BOWEN, A.J. FLAY, R.G.J. PANOFSKY, H.A. — Vertical coherence and phase delay between wind components in strong winds below 20 m. *Boundary-layer Met.*, Vol. 26, pp. 313-324, 1983.

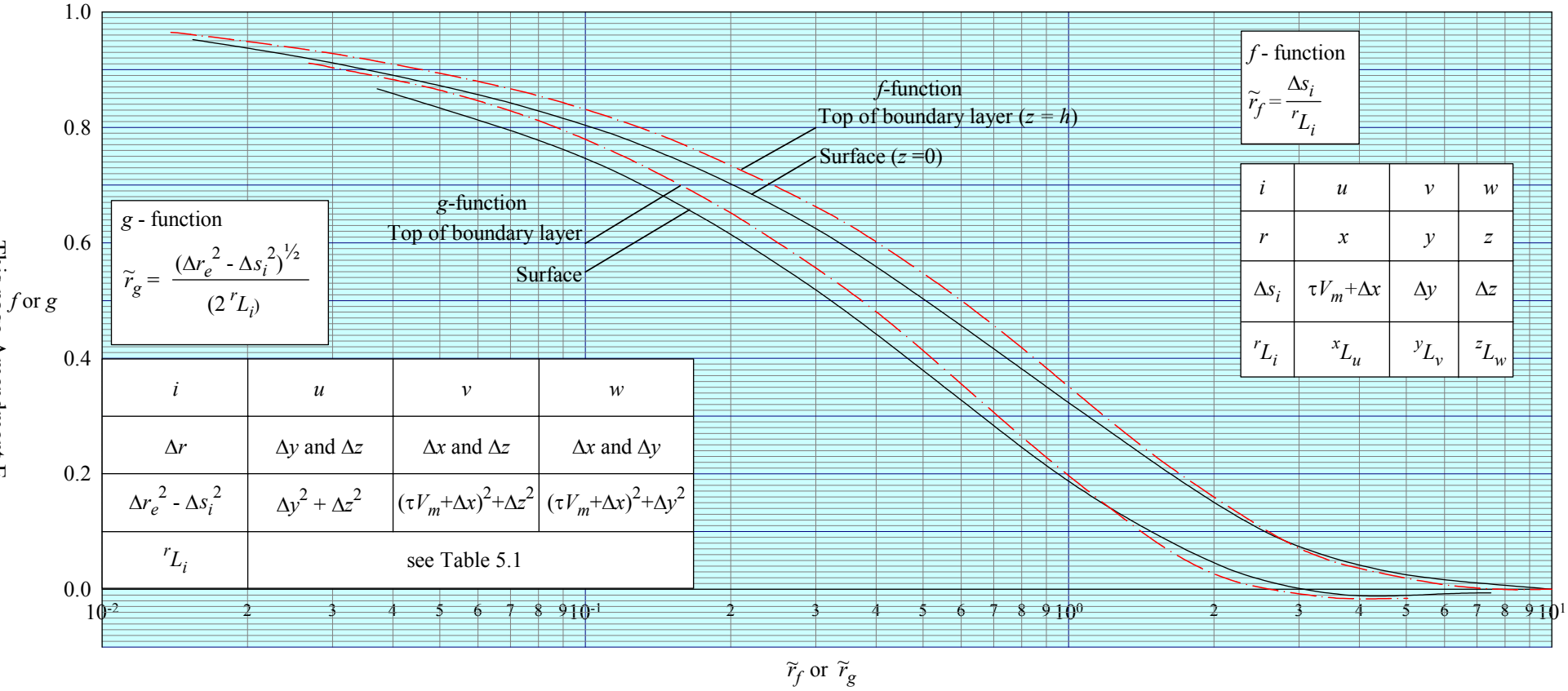

FIGURE 1 CROSS-CORRELATION FUNCTIONS *f* AND *g*

APPENDIX A DERIVATION OF INTEGRAL LENGTH SCALES OF TURBULENCE AND COHERENCE FUNCTIONS

A1. INTEGRAL LENGTH SCALES

A1.1 Derivation of Length Scales from Turbulence Data

Values of the various integral length scales were obtained, where possible, by integrating measured zero-lag cross-correlation functions *i.e.* for $i = u$, v or w and $r = y$ or z.

$$ {}^{r}L_i = \int_0^{\infty} \rho_{ii}\{\Delta r;\, 0\}\, \mathrm{d}(\Delta r)\,. \tag{A1.1} $$

The cases where this procedure can be used are few because of the generally limited number of instrumented stations on a mast; in particular with vertical separations between points different results are obtained depending on whether Δz is increasing upwards or downwards from the reference point. This can be overcome by fitting the appropriate zero-lag cross-correlation function (see Figure 1) to measured values of $\rho_{ii}\{\Delta r\,;0\}$ relating to points z_1 and z_2 and thereby deducing a value of ${}^{z}L_i$ corresponding to the mean height $\tfrac{1}{2}(z_1 + z_2)$. Good agreement was found between values deduced in this way and the few situations where ${}^{r}L_i$ could be obtained through Equation (A1.1). Typical comparisons of measured and predicted zero-lag cross-correlations are shown in Figure A1 using length scales derived in this way.

In general, only those data derived from measurements over uniform terrain were considered although in one case[17] roughness changes exist upwind of a suburban site. However, it is the premise that roughness-change effects on ${}^{x}L_i$ are reflected in the other length scales so that the ratio ${}^{r}L_i/{}^{x}L_u$ is considered to be independent of such influences.

The sources of data used to derive the various length scales are summarised in Table 2.1.

A1.2 Correlation of Length Scale Data

It is reasonable to postulate that the variation of each length scale with wind speed and terrain roughness follows a similar trend to that for the longitudinal length scale, ${}^{x}L_u$. Equations giving the variation of ${}^{x}L_u$ with wind speed, height and terrain roughness are derived in Item 85020 together with relations for ${}^{x}L_v$ and ${}^{x}L_w$ which are

$$ 2\,{}^{x}L_v/{}^{x}L_u = (\sigma_v/\sigma_u)^3\,, \tag{A1.2} $$

$$ 2\,{}^{x}L_w/{}^{x}L_u = (\sigma_w/\sigma_u)^3\,. \tag{A1.3} $$

These follow from the existence of isotropy in the high frequency region and from Equation (A2.19) in Item 85020 which shows that ${}^{x}L_u \propto \sigma_u^3$. (The factor of 2 in Equations (A1.2) and (A1.3) arises from the fact that ${}^{x}L_u$ and ${}^{x}L_w$ are lateral scales, see Section 6.) These relations are confirmed by reliable measurements where both ${}^{r}L_i$ and ${}^{x}L_u$ can be obtained. It follows (and is also justified from measured data) that

$$ {}^{y}L_v/(2\,{}^{y}L_u) = {}^{z}L_v/{}^{z}L_u = (\sigma_v/\sigma_u)^3\,, \tag{A1.4} $$

$$ {}^{y}L_w/{}^{y}L_u = {}^{z}L_w/(2\,{}^{z}L_u) = (\sigma_w/\sigma_u)^3\,. \tag{A1.5} $$

Separate correlations of observed values of ${}^{y}L_u/{}^{x}L_u$ and ${}^{z}L_u/{}^{x}L_u$ with z/h were obtained (Equations (6.7) and (6.8)) and within the scatter of the data were found to be independent of terrain roughness (other than that implied through h). Relations for other length scales in terms of ${}^{x}L_u$ then follow directly from Equations (A1.4) and (A1.5).

Using as a guide the scatter of measured values about the proposed relations for the various length scales, the anticipated uncertainty in predicting any length scale is approximately ±25% . Although this uncertainty may seem large, such a change in ${}^{r}L_i$ has a much smaller effect on the prediction of $\rho_{ii}\{\Delta r\}$ and coherence values.

The effect of wind strength on ${}^{x}L_u$ (and hence on all other length scales) must be emphasised. Most measurements are made at moderate wind speeds (typically $V_{10} = 8$ to 13 m/s) whereas design wind speeds are in the range $V_{10} = 20$ to 35 m/s. **The result of this is that length scales for design purposes are very much larger than typical values reported in the literature.**

A2. DERIVATION OF COHERENCE FUNCTIONS

The most common form of empirical expression used to represent measured coherence data is a simple exponential function of the form

$$\sqrt{\text{coherence}} = \gamma_{ii}\{\Delta r\} = \exp(-a_{ii} n\, \Delta r/V_m)\,. \tag{A2.1}$$

This expression has limitations (as summarised in Section 7.1) in representing the data, not the least of which is the fact that a_{ii} is not truly a constant but varies with frequency. The von Karman model for isotropic turbulence provides theoretically based equations for the coherence functions which fit measured data well but only for comparatively large heights above the ground when the condition of isotropy is approached. However, physically, the equations are well based and for this reason they form the basis of the model derived for this Item but with modifications to account for the departure from isotropic conditions nearer the ground.

The von Karman equations for coherence, applicable to isotropic turbulence are as follows. For the u-component with separations $\Delta r = \Delta y$ or Δz, the root-coherence function is given by

$$\gamma_{uu}\{\Delta r\} = 0.994[\eta^{5/6}K_{5/6}\{\eta\} - \tfrac{1}{2}\eta^{5/3}(\eta^{1/6}K_{1/6}\{\eta\})] \tag{A2.2}$$

where

$$\eta = \left[\left(\frac{0.747\Delta r}{L}\right)^2 + \left(\frac{2\pi n \Delta r}{V_m}\right)^2\right]^{1/2} \tag{A2.3}$$

and L is the longitudinal length scale.

For the v- and w-components with separations $\Delta r = \Delta y$ or Δz (i denotes v or w)

$$\gamma_{ii}\{\Delta r\} = \frac{0.597}{\{(2.869\eta^2)/(\Delta r/L)^2\} - 1}\left[\frac{4.781\eta^2}{(\Delta r/L)^2}\eta^{5/6}K_{5/6}\{\eta\} - \eta^{11/6}K_{11/6}\{\eta\}\right] \tag{A2.4}$$

with η given by Equation (A2.3).

In Equations (A2.2) and (A2.4) the $K_v(\eta)$ functions are modified Bessel functions of the second kind; Figures A2 and A3 show a plot of each coherence function against the non-dimensional parameter η. Note

that above the very low frequency range η approximates closely to

$$\eta = 2\pi n\ \Delta r/V_m\,. \tag{A2.5}$$

Good working approximations to these relations are given by the much simpler equations

$$\gamma_{uu}\ \{\Delta r\} = \exp[-1.15\ \eta^{1.5}] \tag{A2.6}$$

and for $i = v$ or w

$$\gamma_{ii}\ \{\Delta r\} = \exp[-0.65\ \eta^{1.3}] \tag{A2.7}$$

and these are also shown on Figures A2 and A3.

A modification to Equations (A2.6) and (A2.7) was sought to account for the departure, near the ground, from the isotropic relationships. The supposition was made that the foregoing equations could still be applied but using a transformed η (to η_1) that would reflect the distorting effects due to the ground. It was reasoned that this transformation would be dependent on the separation distance in relation to the typical size of turbulent eddies, *i.e.* on $\Delta r/{}^{r}L_i$. Furthermore, since the properties of turbulence at high frequencies tend to regain the characteristics of isotropy, the transformation η_1/η should tend to unity as n increases. From physical considerations this functional dependence was reasoned to be the ratio of the wavelength of turbulence (V/n) to the separation distance (Δr), *i.e.* as $n\Delta r/V$ increases the transformation η_1/η should tend to unity. In addition, if this concept is to be physically acceptable the transformation should apply universally to all three components (u, v and w) and to separations in any lateral direction.

Using data from those sources where coherence data for individual runs were presented, a transformed η of the form

$$\eta_1 = \left[\left\{\frac{0.747\Delta r}{2^{r}L_i}\right\}^2 + \left\{c\frac{2\pi n\Delta r}{V_m}\right\}^2\right]^{1/2} \tag{A2.8}$$

was found to be apply universally. In Equation (A2.8), $2^{r}L_i$ is twice the lateral length scale (appropriate to a mean height and mean wind speed between points separated by Δr for the terrain in question) in place of the isotropic length scale, L. The parameter c transforms the wavelength of turbulence to an equivalent wavelength in "iso-space" where Equations (A2.6) and (A2.7) are applicable. Using measurements (see Table 2.1) for the u- and v- components with separations in the y- and z- directions, a general empirical relationship for c was found to be

$$c = 1.6[\Delta r/(2^{r}L_i)]^{0.13}/\eta^{b} \ \text{ or } 1.0 \tag{A2.9}$$

whichever is the greater, with

$$b = 0.35\ [\Delta r/(2^{r}L_i)]^{0.2}\,, \tag{A2.10}$$

where η is given by Equation (A2.3) with $L = 2^{r}L_i$ and ${}^{r}L_i$ is given by the appropriate relation in Section 6. Note that as n increases, or $\Delta r/(2^{r}L_i)$ decreases, $c \to 1.0$.

As mean wind speed (for a given height and terrain) increases the effect is to increase $\gamma_{ii}\{\Delta r\}$. In the present ESDU model the appropriate length scale (${}^{r}L_i$) also increases with wind speed and the overall effect is to increase c resulting in a smaller increase in $\gamma_{ii}\{\Delta r\}$ than would have been obtained using an equation in which the anisotropic effects (dependent on $\Delta r/{}^{r}L_i$) are not correctly modelled.

The transformed model was found to provide very good agreement with good quality data as illustrated by the typical comparisons with measurements in Figures A4 and A5. In comparing data for the v-component, the co-coherence (in-phase) component is presented; this is obtained from $\gamma_{vv}\{\Delta r\}$ using Equations (7.13) and (7.14) with $\theta_{vv}\{\Delta z\}$ given by Equation (7.18).

Only limited data are available for the w-component with separations in the y-direction. Data[9] for wind from the sea, approximately normal to a line of anemometers at $z = 40$ m for a particular run is shown in Figure A6 together with a prediction using the present method. Despite the scatter of the measured data the agreement is good and it is reasonable to suggest that the applicability of the models presented is general, especially to the design situation when wind speeds are much higher than those at which measured data are available.

Further comparisons with measured data are discussed in Section A2.1.

A2.1 Comparison with the Simple Exponential Model

Many of the data in the literature relating to coherence measurements are presented in the form of decay constants, a_{ii}, for use with the exponential equation

$$\gamma_{ii}\{\Delta r\} = \exp[-a_{ii} n\, \Delta r/V_m]. \tag{A2.11}$$

A comparison of the present ESDU model with these data is possible by equating Equation (A2.11) with the equations derived in Section A2 which are of the general form

$$\gamma_{ii}\{\Delta r\} = \exp[-D\eta_1{}^{B}]. \tag{A2.12}$$

The resulting expression for a_{ii} is

$$a_{ii} = \frac{D}{N}(0.747\tilde{r}_g)^B \left\{ 1 + \frac{4.588(2\pi N)^{2-2b}}{\tilde{r}_g{}^{1.74}(1 + 0.01413\tilde{r}_g^2/N^2)^b} \right\}^{B/2} \tag{A2.13}$$

where $N = n\Delta r/V_m$, $\tilde{r}_g = \Delta r/(2^{r}L_i)$ and b is given by Equation (A2.10). Thus, it is clear that a_{ii} is dependent on the value of $n\Delta r/V_m$ at which the fit for a_{ii} is made and on the parameter $\Delta r/(2^{r}L_i)$. Most values of a_{ii} reported in the literature are obtained over the range $0 \le N \le 0.1$ so that for a given N (= 0.05 say) Equation (A2.13) reduces to a function of $\Delta r/(2^{r}L_i)$ only. Figure A7 gives the relationship between a_{ii} and $\Delta r/(2^{r}L_i)$ for the u-component ($D = 1.15$, $B = 1.5$) and for the v-component ($D = 0.65$, $B = 1.3$). These relations were obtained using $N = 0.05$ and then curve fitting to obtain the equations (plotted in Figure A7).

$$a_{uu}\{\Delta r\} = 6.2 + 14.2\,[\Delta r/2^{r}L_u)]^{0.96}, \tag{A2.14}$$

$$a_{vv}\{\Delta z\} = 3.6 + 8.1\,[\Delta z/2^{z}L_v)]^{0.96}. \tag{A2.15}$$

It should be remembered that the simple exponential expression (Equation (A2.11)) for $\gamma_{ii}(\Delta r)$ tends to unity as $n\ \Delta r/V_m$ tends to zero which leads to small errors for the *u*-component but much larger errors for the *v*- and *w*-components (particularly the latter) as described in Section 7.1. This makes a comparison with Equation (A2.11) inappropriate for the *w*-component.

Values of a_{ii} in the literature tend to be correlated with the parameter $\Delta r/z$ rather than $\Delta r/(2^rL_i)$. However, since most of the data are for relatively smooth terrain and for a small range of wind speeds around V_{10} = 10 m/s, it follows that ^rL_i, to a first approximation, is a function of z only in these cases. It is thus not surprising that a correlating trend between a_{ii} and $\Delta r/z$ can be made, albeit with considerable scatter. Examples of such correlations of data[21] are shown in Figure A8, most of the data being obtained for heights less than about 40 m. Superimposed on these correlations are values obtained from Figure A7 for various mean heights assuming open country terrain and V_{10} = 10 m/s to obtain ^rL_i. It is clear that there is general agreement between the two sets of data and that some of the scatter in the experimental values of a_{ii} is due to using $\Delta z/z$, rather than $\Delta z/(2^zL_i)$, as the correlating parameter.

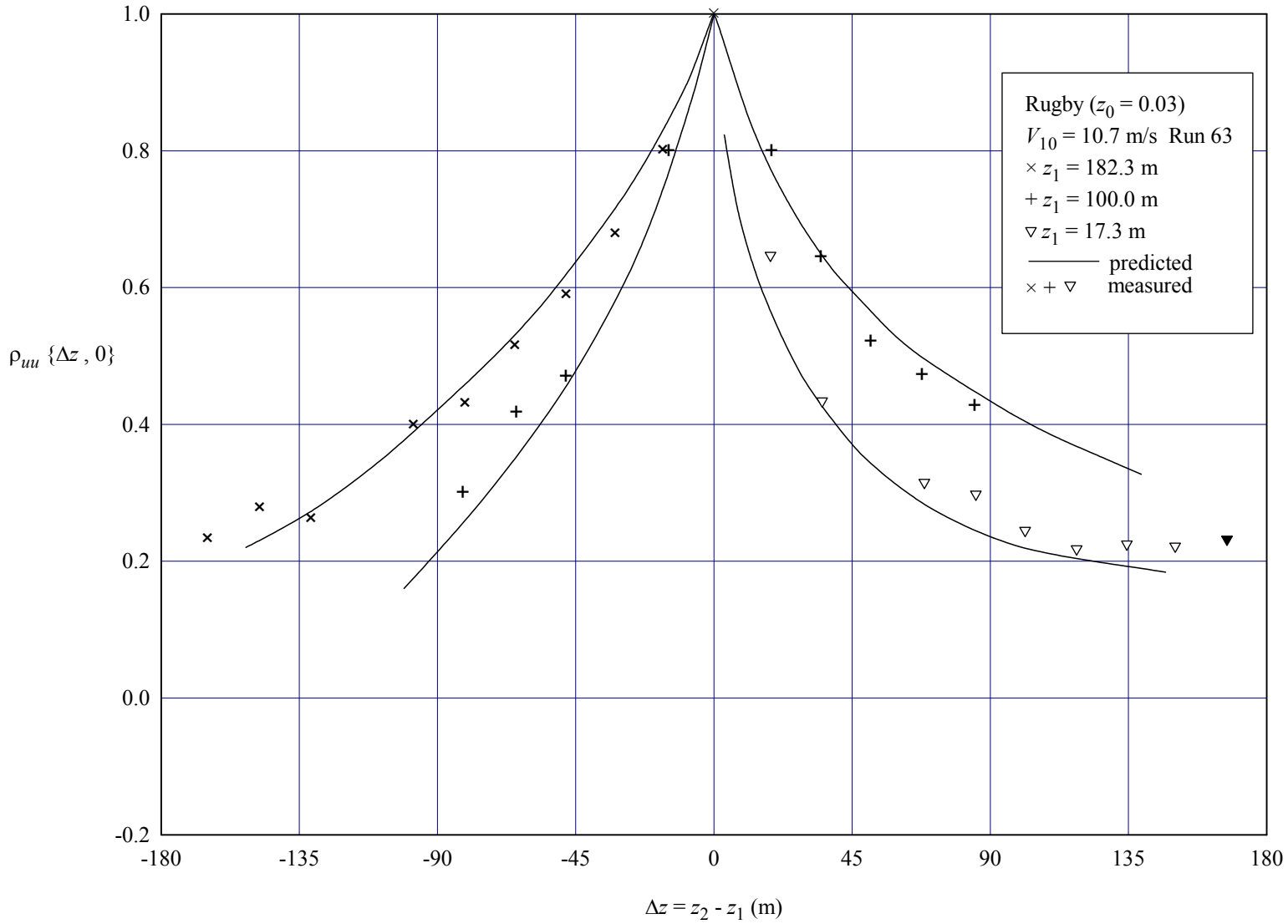

FIGURE A1 TYPICAL COMPARISON OF PREDICTED AND MEASURED ZERO-LAG CROSS-CORRELATIONS FOR *u*-COMPONENTS WITH VERTICAL SEPARATIONS

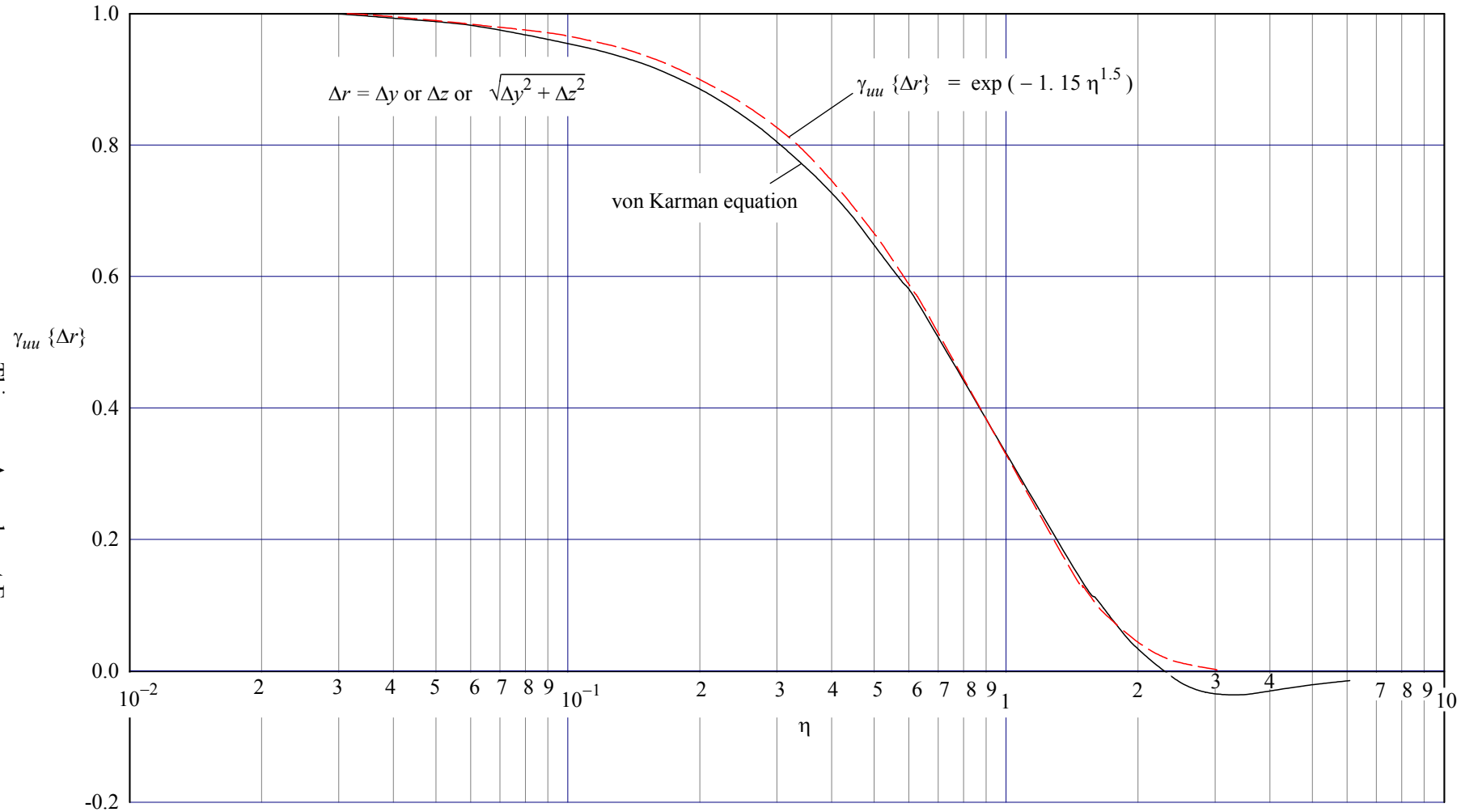

FIGURE A2 $\sqrt{\text{COHERENCE}}$ FUNCTION FOR *u*-COMPONENTS WITH TRANSVERSE SEPARATIONS

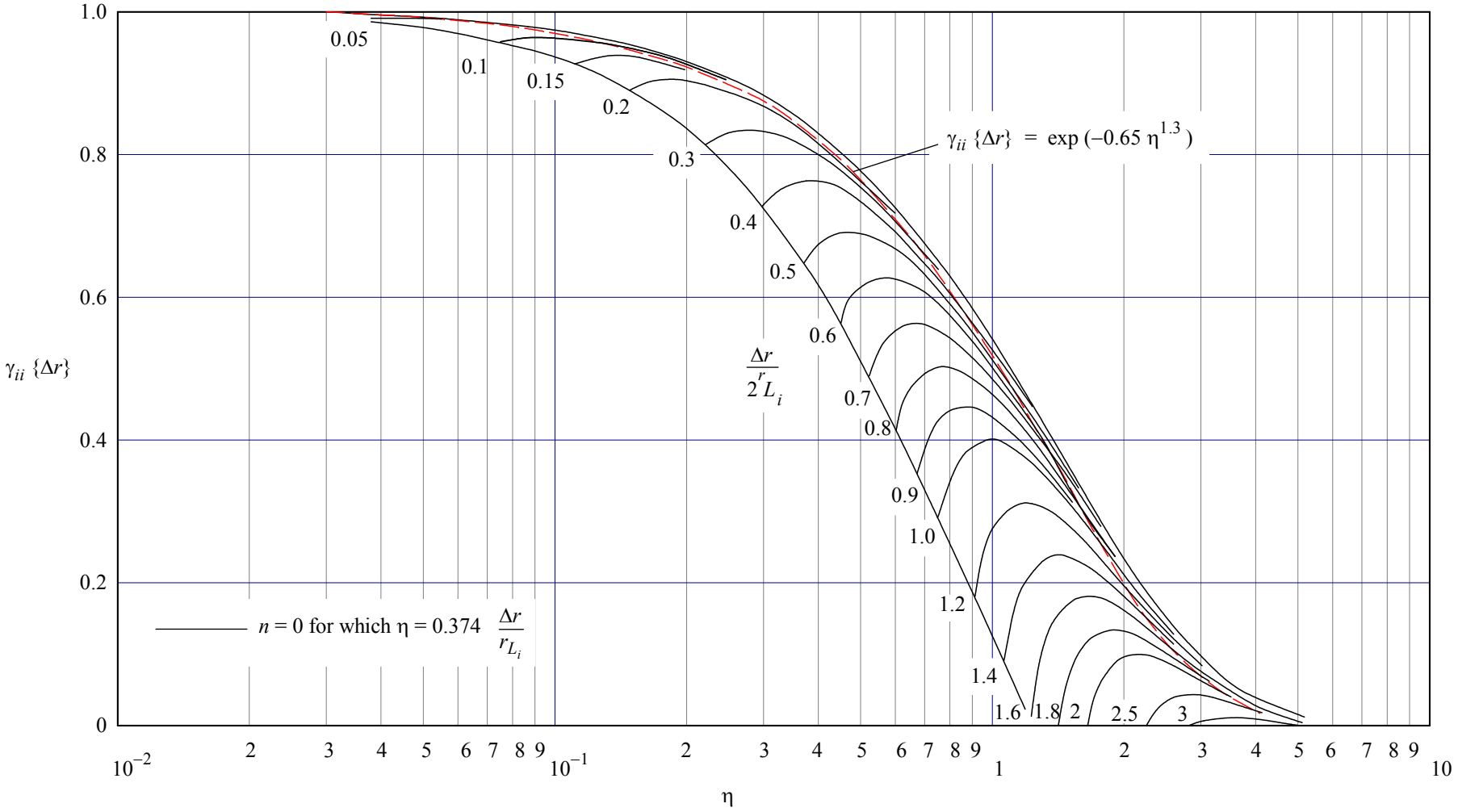

FIGURE A3 $\sqrt{\text{COHERENCE}}$ FUNCTION FOR *v*- AND *w*- COMPONENTS WITH VERTICAL AND LATERAL SEPARATIONS RESPECTIVELY

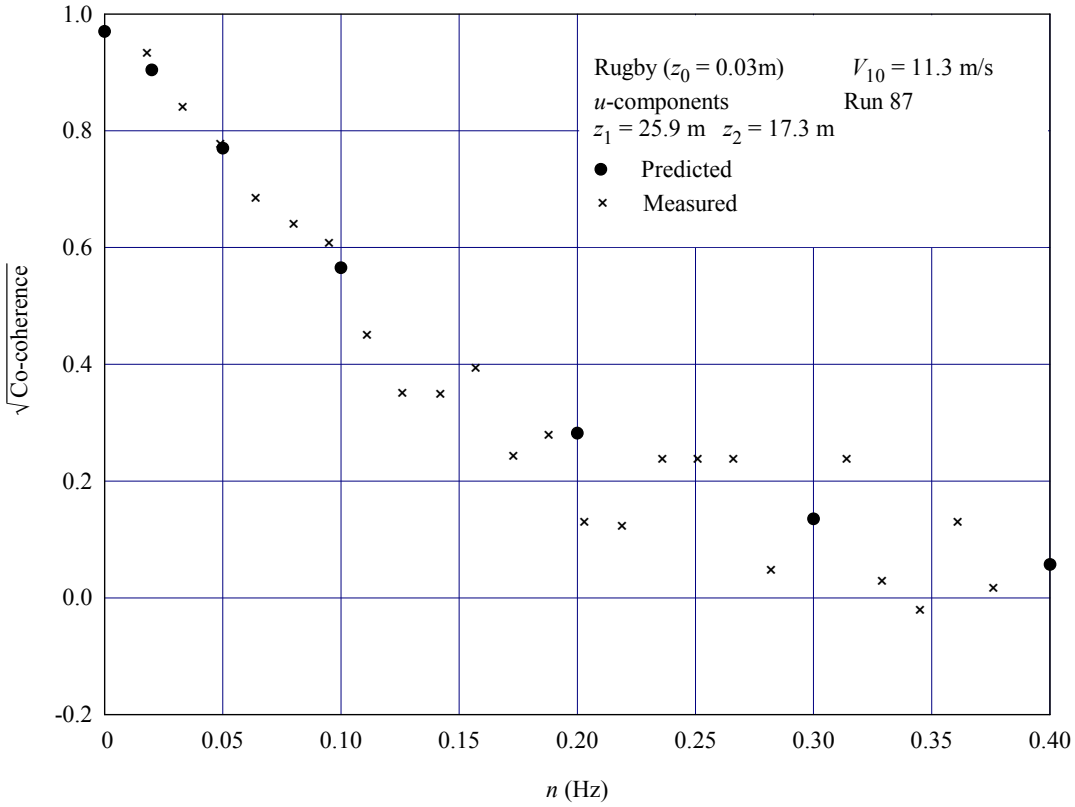

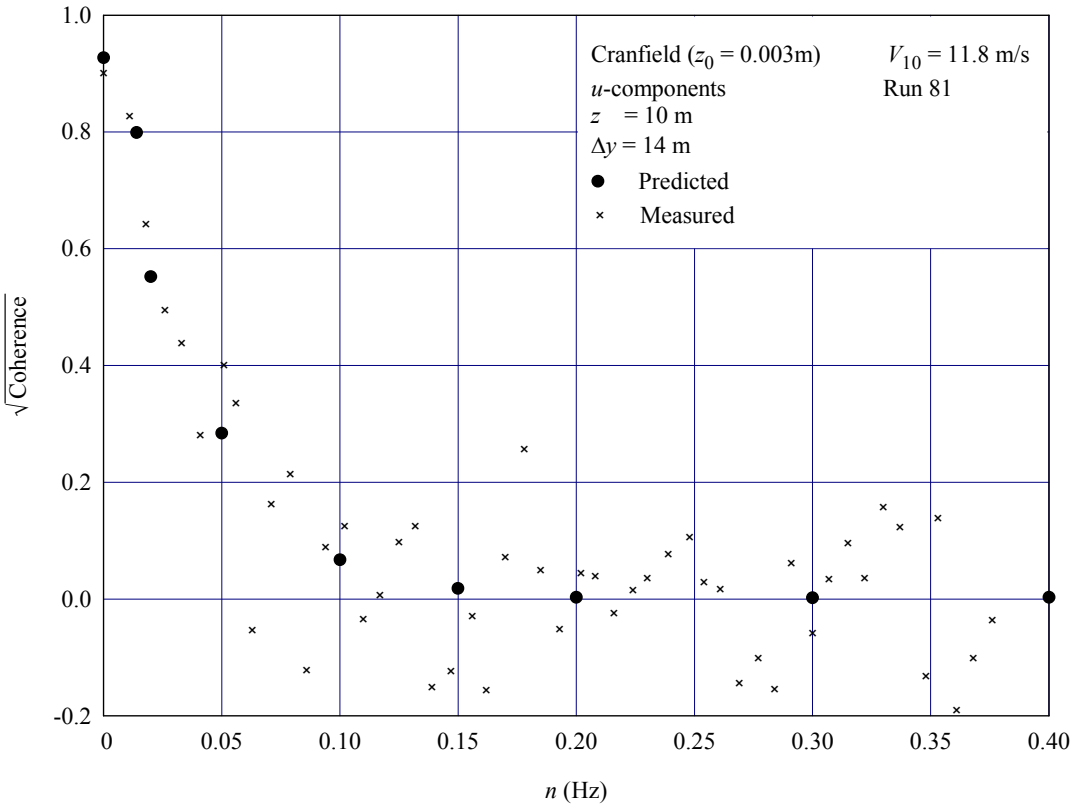

FIGURE A4 TYPICAL COMPARISONS OF PREDICTED AND MEASURED COHERENCE DATA FOR *u*-COMPONENTS

This page Amendment E

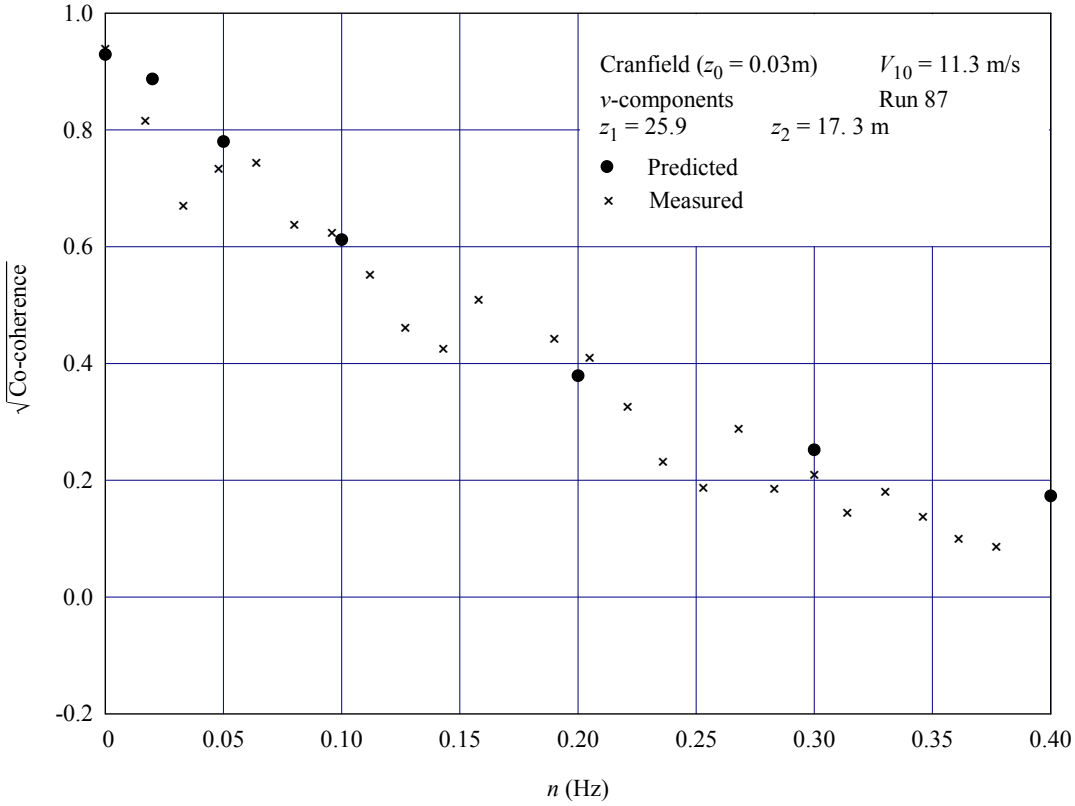

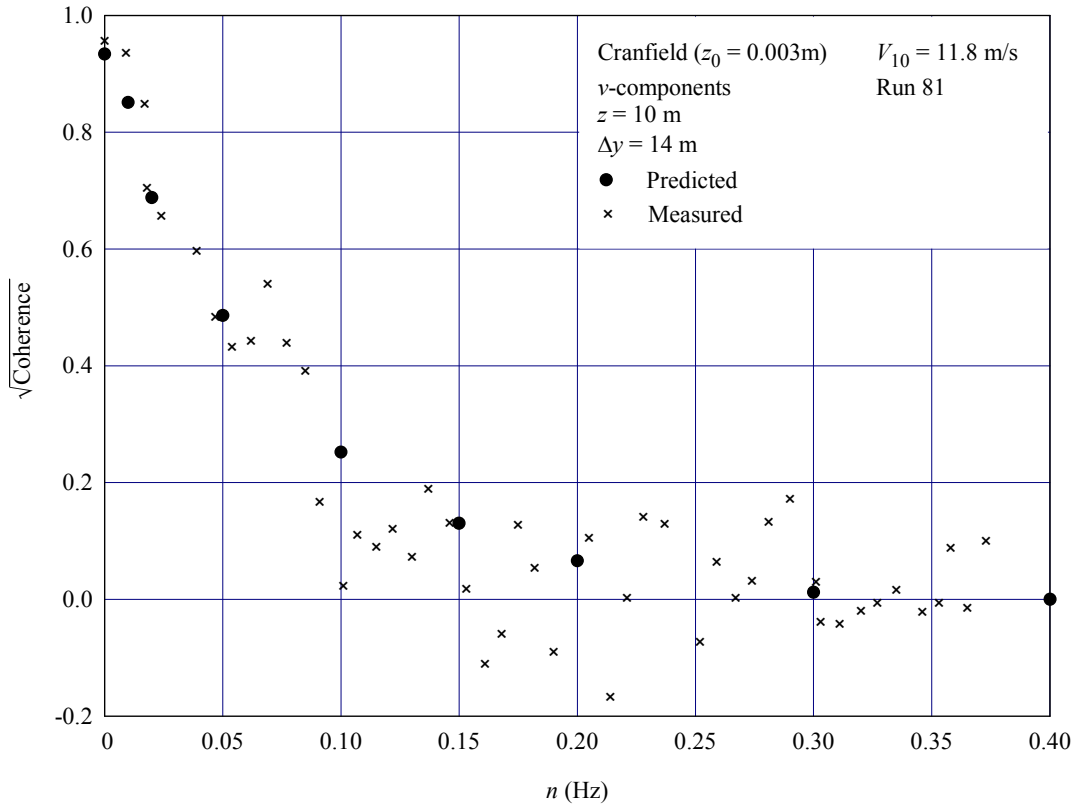

FIGURE A5 TYPICAL COMPARISONS OF PREDICTED AND MEASURED COHERENCE DATA FOR *v*-COMPONENTS

This page Amendment E

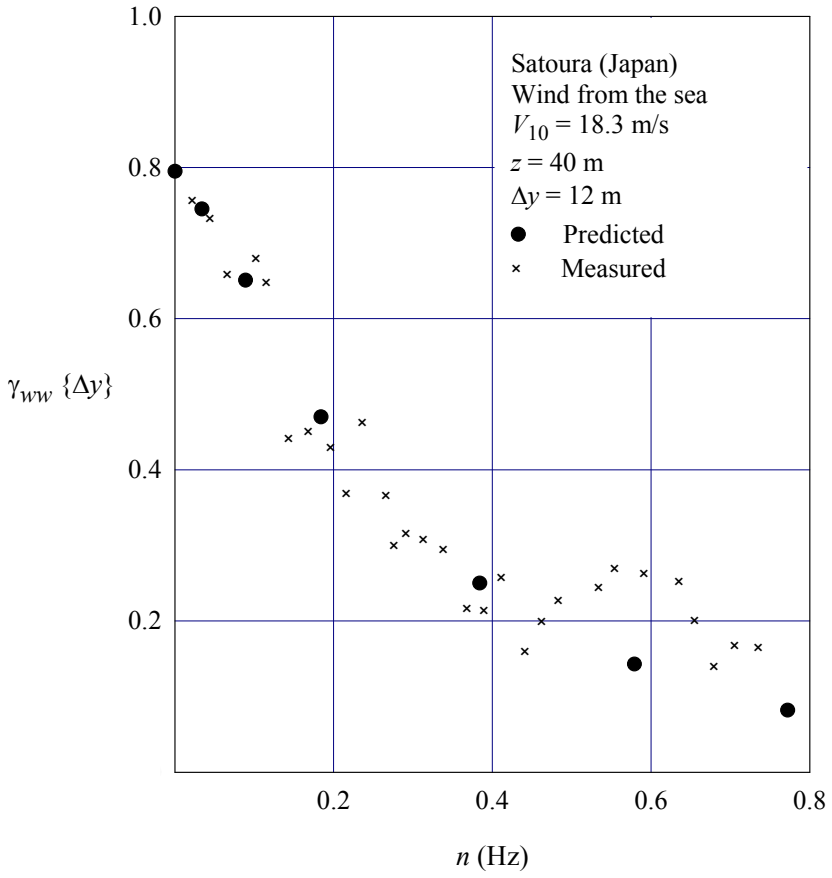

FIGURE A6 COMPARISON OF PREDICTED AND MEASURED COHERENCE DATA FOR *w*-COMPONENTS

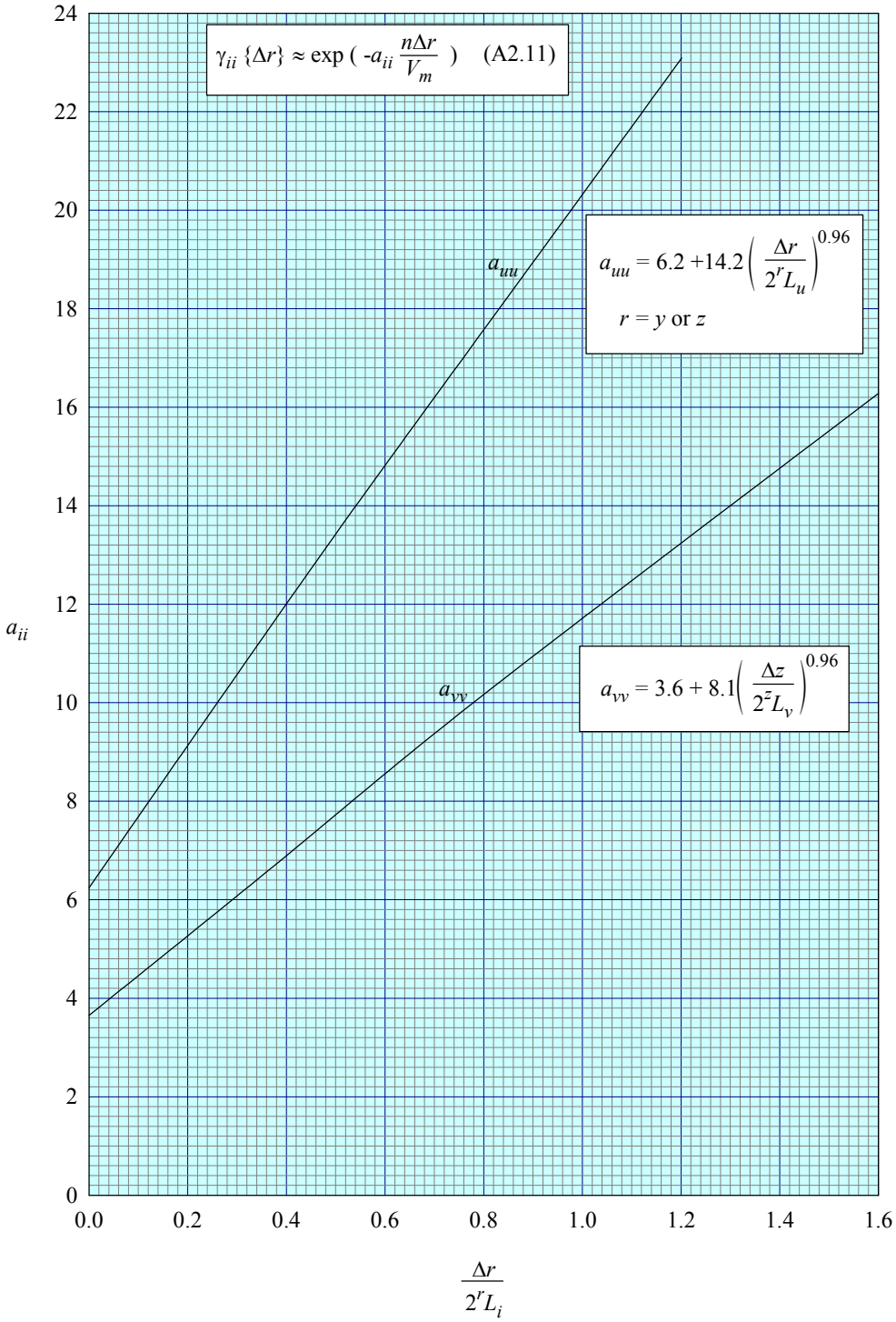

FIGURE A7 VALUES OF DECAY CONSTANT USED IN EQUATION (A2.11)

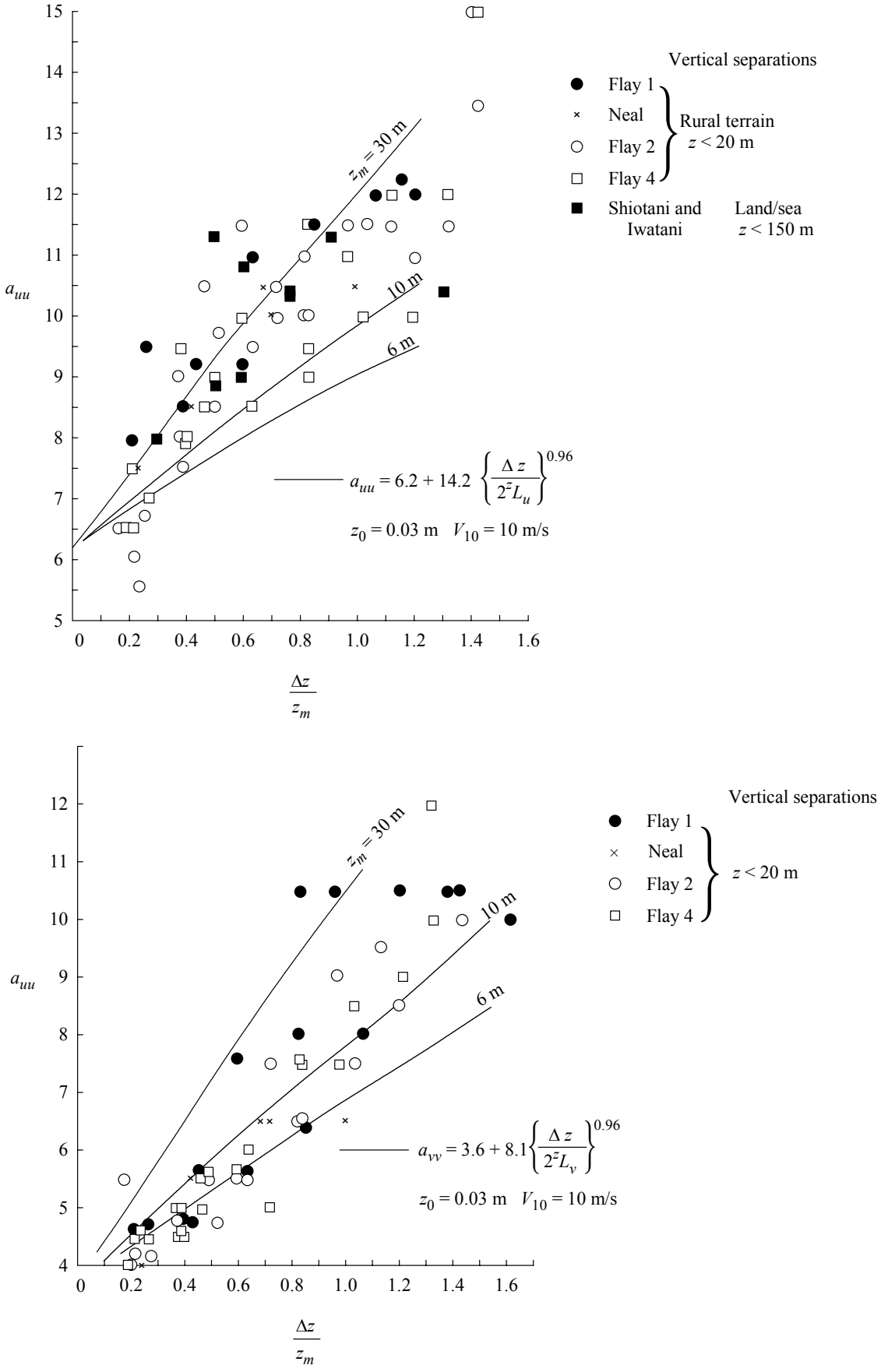

FIGURE A8 COMPARISONS OF PREDICTED AND MEASURED VALUES OF THE EXPONENTIAL DECAY CONSTANT AS USED IN EQN (A2.11)

KEEPING UP TO DATE

Whenever Items are revised, subscribers to the service automatically receive the material required to update the appropriate Volumes. If you are in any doubt as to whether or not your ESDU holding is up to date, please contact us.

Please address all technical engineering enquiries and suggestions to:

ESDU International plc	Tel:	020 7490 5151 (from the UK)
		+44 20 7490 5151 (from outside the UK)
	Fax:	020 7490 2701 (from the UK)
		+44 20 7490 2701 (from outside the UK)
	E-Mail:	esdu@esdu.com
	Website:	www.esdu.com

For users in the USA, please address all Customer Service and Support enquiries and suggestions to:

IHS Engineering Products	Tel:	1 800 525 7052 (toll free number)
and	Fax:	1 303 397 2599
Global Engineering Documents	Website:	www.ihs.com www.global.ihs.com

ESDU 86010

Characteristics of atmospheric turbulence near the ground
Part III: variations in space and time for strong winds (neutral atmosphere)
ESDU 86010

ISBN 0 85679 562 3, ISSN 0143-2702

Available as part of the ESDU Series on Wind Engineering. For information on all ESDU validated engineering data contact ESDU International plc, 27 Corsham Street, London N1 6UA.

The properties of turbulence in the atmospheric wind are important in estimating wind loading effects. Typical applications are aircraft response prediction, the estimation of peak loadings on ground-based structures and scale modelling in atmospheric boundary layer wind-tunnel testing.

ESDU 86010 (which supersedes ESDU 75001) is part of a series of Items providing the most comprehensive set of turbulence characteristics for the atmospheric boundary layer in strong winds (neutral atmosphere). This part deals with the spatial properties of the longitudinal (u), lateral (v) and vertical (w) components of fluctuating wind speed measured at two points in space.

The properties covered are joint probability, cross-correlations, coherence and phase angle (giving cross-spectral densities) and integral length scales of turbulence of all components in any direction. The data are applicable throughout the atmospheric boundary layer and different types of terrain. The length scales are all related to the longitudinal value ${}^{x}L_u$ and scaled according to similarity rules in the atmospheric boundary layer; they are therefore dependent on wind strength. Roughness changes upwind of a site can be accounted for by the effect on ${}^{x}L_u$ as described in ESDU 85020 giving single point data.

The data are derived from the von Kármán equations modified to account for the distorting (anisotropic) effect near the ground. The theoretical basis allows a rational extrapolation from measurements obtained at moderate wind speeds to the much higher design wind speed case when, in particular, much larger length scales are obtained.